

Supporting Information

Calorimetric Analysis of the Interplay between Synthetic Tn Antigen-presenting MUC1 Glycopeptides and Human Macrophage Galactose-type Lectin

Donella M. Beckwith¹, Forrest G. FitzGerald^{1†}, Maria C. Rodriguez Benavente^{1δ}, Elizabeth R. Mercer¹, Anna-Kristin Ludwig², Malwina Michalak³, Herbert Kaltner², Jürgen Kopitz³, Hans-Joachim Gabius², and Maré Cudic^{1}*

¹Florida Atlantic University, Department of Chemistry and Biochemistry, Charles E. Schmidt College of Science, Boca Raton, FL 33431, United States

²Ludwig-Maximilians-University Munich, Institute of Physiological Chemistry, Faculty of Veterinary Medicine, Veterinärstr. 13, 80539 Munich, Germany

³Department of Applied Tumor Biology, Institute of Pathology, Medical School of the Ruprecht-Karls-University Heidelberg, Im Neuenheimer Feld 224, 69120 Heidelberg, Germany

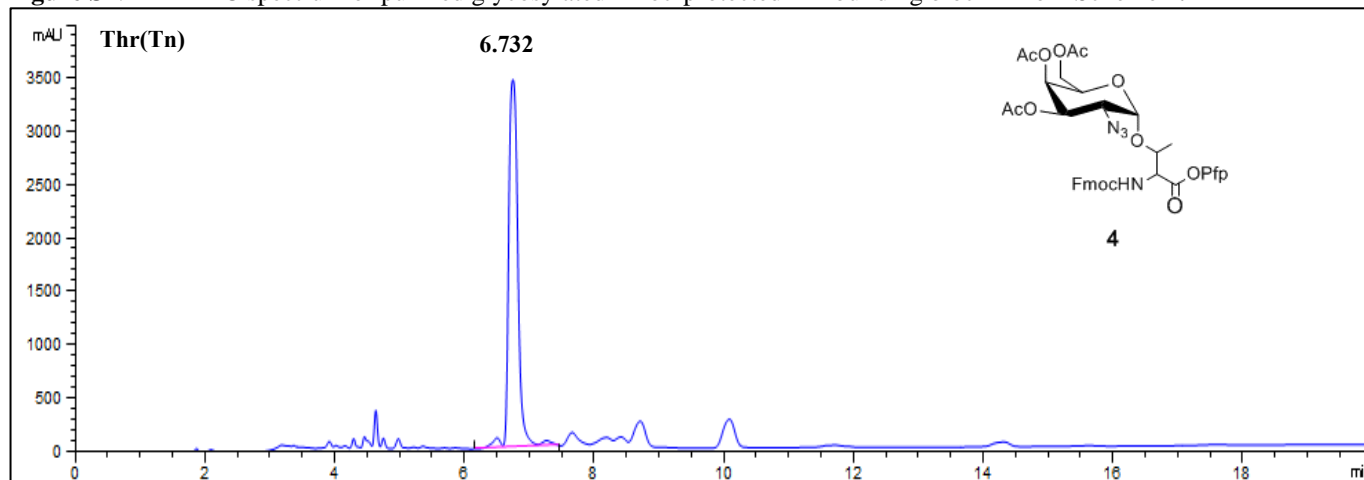
Table of Contents

Page	Content
S1&S2	Title page and table of contents.
S3	Figure S1. RP-HPLC chromatogram of purified glycosylated Fmoc-protected Thr building block 4 derived from Scheme 1. Figure S2. MALDI-TOF mass spectrum of purified glycosylated Fmoc-protected Thr building block 4 .
S4	Figure S3. ¹ H NMR spectrum of purified glycosylated Fmoc-protected Thr building block 4 . Figure S4. ¹³ C NMR spectrum of purified glycosylated Fmoc-protected Thr building block 4 .
S5	Figure S5. RP-HPLC chromatogram of purified glycosylated Fmoc-protected Thr building block 5 derived from Scheme 1. Figure S6. MALDI-TOF mass spectrum of purified glycosylated Fmoc-protected Thr building block 5 .

Page	Content
S6	Figure S7. ¹ H NMR spectrum of purified glycosylated Fmoc-protected Thr building block 5 . Figure S8. ¹³ C NMR spectrum of purified glycosylated Fmoc-protected Thr building block 5 .
S7	Figure S9. General synthesis scheme of glycopeptides.
S8	Figure S10. RP-HPLC chromatogram of purified MUC1 (6). Figure S11. MALDI-TOF mass spectrum of purified MUC1 (6).
S9	Figure S12. RP-HPLC chromatogram of purified MUC1-Thr4 (7). Figure S13. MALDI-TOF mass spectrum of purified MUC1-Thr4 (7).
S10	Figure S14. RP-HPLC chromatogram of purified MUC1-Thr9 (8). Figure S15. MALDI-TOF mass spectrum of purified MUC1-Thr9 (8).
S11	Figure S16. RP-HPLC chromatogram of purified MUC1-Thr16 (9). Figure S17. MALDI-TOF mass spectrum of purified MUC1-Thr16 (9).
S12	Figure S18. RP-HPLC chromatogram of purified MUC1-Thr9,16 (10). Figure S19. MALDI-TOF mass spectrum of purified MUC1-Thr9,16 (10).
S13	Figure S20. RP-HPLC chromatogram of purified MUC1-Thr4,16 (11). Figure S21. MALDI-TOF mass spectrum of purified MUC1-Thr4,16 (11).
S14	Figure S22. RP-HPLC chromatogram of purified MUC1-Thr4,9 (12). Figure S23. MALDI-TOF mass spectrum of purified MUC1-Thr4,9 (12).
S15	Figure S24. RP-HPLC chromatogram of purified MUC1-Thr4, 9,16 (13). Figure S25. MALDI-TOF mass spectrum of purified MUC1-Thr4,9, 16 (13).
S16	Figure S26. Circular dichroism (CD) spectrum of MUC1 (glycol)peptides in buffered (A) water (H ₂ O) and (B) deuterium oxide (D ₂ O).
S17	Figure S27A. Molecular mass determination of hMGL by MALDI-TOF mass spectrum.
S18	Figure S27B. Tryptic peptide mass fingerprinting of hMGL by MALDI-TOF mass spectrum.
S19	Figure S27C. Chymotryptic peptide mass fingerprinting of hMGL by MALDI-TOF mass spectrum.
S20	Figure S27D. Combined sequence coverage of tryptic and chymotryptic peptide mass fingerprinting of hMGL by MALDI-TOF mass spectrum.
S21	Figure S28. ITC titration profiles and signature plots of (A) α/β-GalNAc, (B) Thr-Tn, (C) α-Me-GalNAc, and (D) β-Me-GalNAc with hMGL in buffered water and ITC signature plots.
S22	Figure S29. ITC titration profiles of (A) MUC1-Thr4, (B) MUC1-Thr9, and (C) MUC1-Thr16 with hMGL in buffered water.
S23	Figure S29. ITC titration profiles of (D) MUC1-Thr9,16, (E) MUC1-Thr4,16, (F) MUC1-Thr4,9, and (G) MUC1-Thr4,9,16 with hMGL in buffered water and ITC signature plots.
S24	Figure S30. ITC titration profiles of (A) MUC1-Thr4, (B) MUC1-Thr9, and (C) MUC1-Thr16 with hMGL in buffered deuterium oxide.
S25	Figure S30. ITC titration profiles of (D) MUC1-Thr9,16, (E) MUC1-Thr4,16, (F) MUC1-Thr4,9, and (G) MUC1-Thr4,9,16, with hMGL in buffered deuterium oxide and ITC signature plots.
S26	Figure S31. NITPIC/SEDPHAT thermodynamic values in water.
S27	Figure S31. NITPIC/SEDPHAT thermodynamic values in deuterium oxide.
S28	Figure S32. AFFINImeter KinITC data in water.
S29	Figure S33. AFFINImeter KinITC data in deuterium oxide.

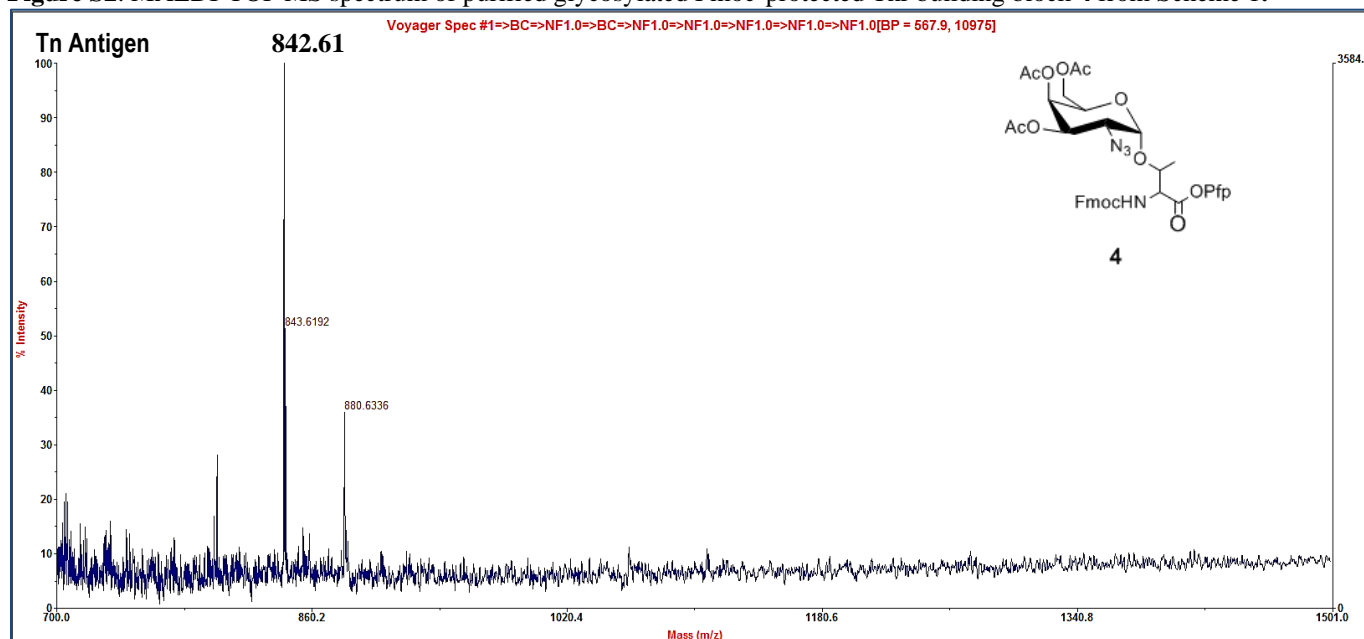
Thr-Azide

Figure S1. RP-HPLC spectrum of purified glycosylated Fmoc-protected Thr building block **4** from Scheme 1.



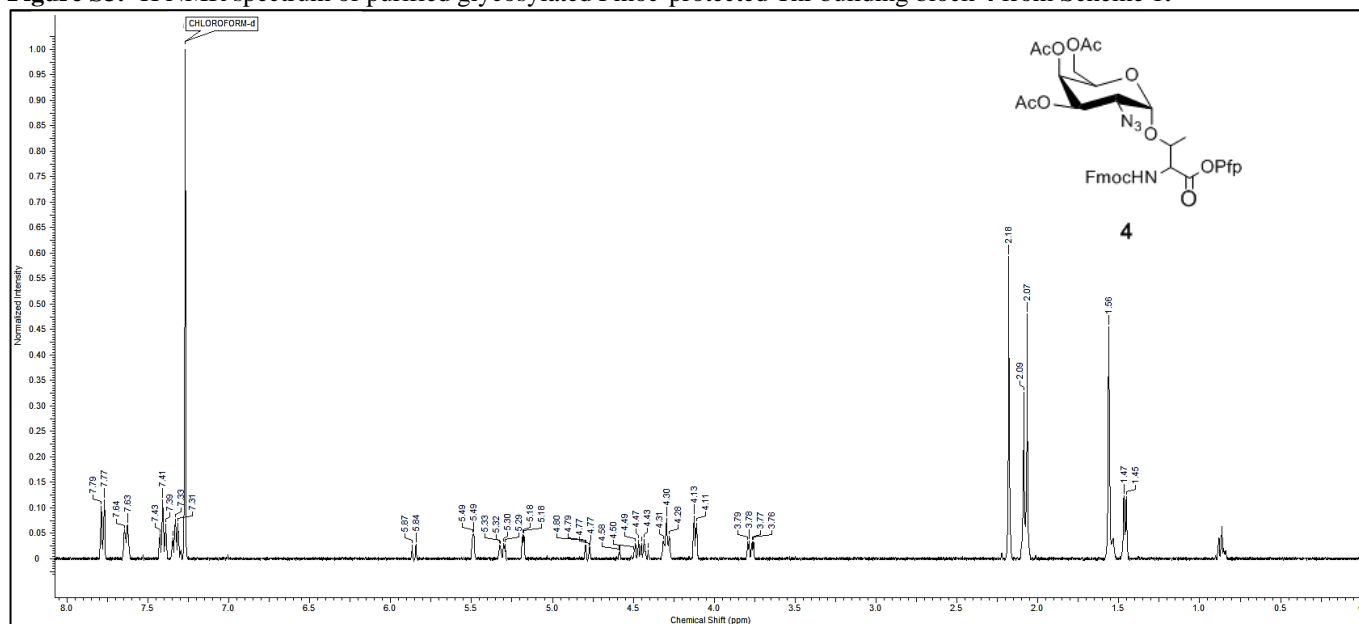
HPLC analysis of purified glycosylated Fmoc-protected Thr building block **4** derived from Scheme 1. Eluents were 0.1% TFA in water (A) and 0.1% TFA in acetonitrile (B). The elution gradient was 60-100% B in 20 mins with a flow rate of 1.0 mL/min. Detection was at wavelength = 214 nm. Retention time (min) = 6.732.

Figure S2. MALDI-TOF MS spectrum of purified glycosylated Fmoc-protected Thr building block **4** from Scheme 1.



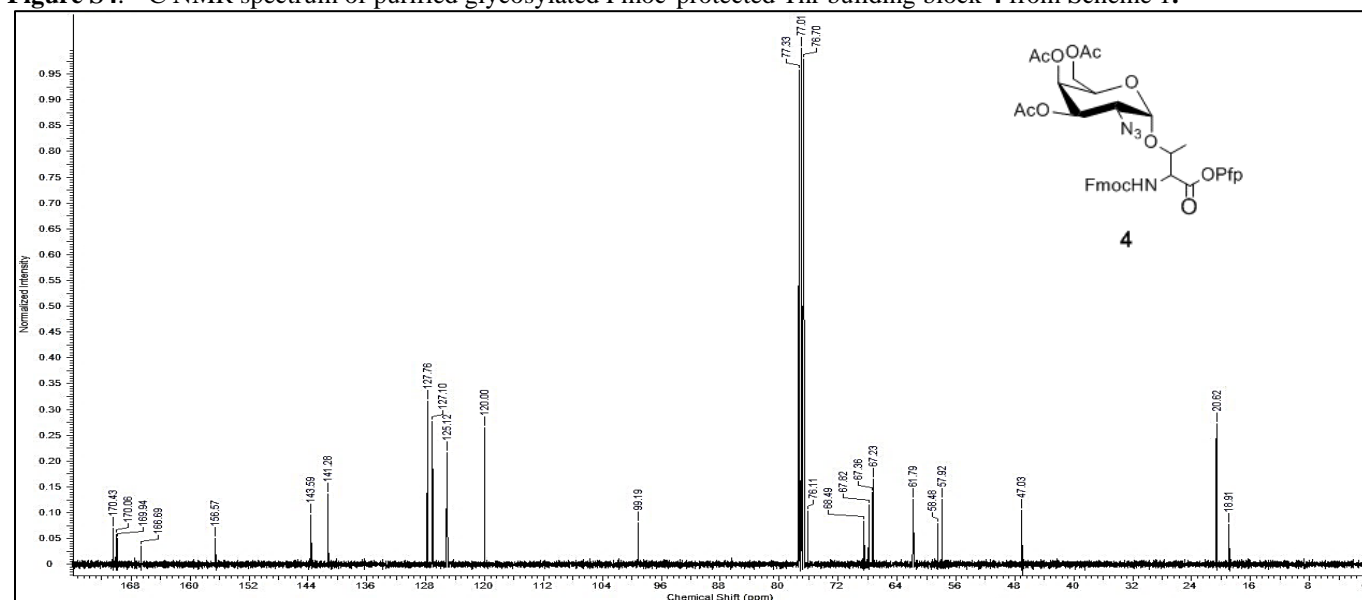
MALDI-TOF MS analysis of purified glycosylated Fmoc-protected Thr building block **4** derived from Scheme 1. Thr-Azide: $[M + Na]^+ = 842.61$ Da (expected, 843.66 Da).

Figure S3. ^1H NMR spectrum of purified glycosylated Fmoc-protected Thr building block **4** from Scheme 1.



^1H NMR (400 MHz, CDCl_3): δ [ppm] = 7.78-7.76 (d, $J=7.4$ Hz, Ar-H Fmoc, 2H), 7.63-7.62 (d, $J=6.5$ Hz, Ar-H Fmoc, 2H), 7.42-7.38 (m, Ar-H Fmoc, 2H), 7.34-7.30 (m, Ar-H Fmoc, 2H), 5.87-5.84 (d, $J=9.0$ Hz, HN-Thr, 1H), 5.49 (d, $J=3.0$ Hz, Gal-H₄, 1H), 5.33-5.29 (dd, $J=11.0$ Hz, Gal-H₃, 1H), 5.18 (d, $J=3.5$ Hz, Gal- α H₁, 1H), 4.80-4.77 (dd, $J=10.7$ Hz, Thr- α H, 1H), 4.59 (m, Thr- β H, 1H), 4.49-4.43 (m, Fmoc-CH₂, 2H), 4.31-4.28 (t, Fmoc-CH and Gal-H₅, 2H), 4.13-4.11 (dd, $J=6.0, 1.5$ Hz, Gal-H_{6a-6b}, 2H), 3.79-3.76 (dd, Gal-H₂, 1H), 2.17-2.07 (3s, COCH₃, 9H), 1.47-1.45 (d, $J=6.0$ Hz, Thr-CH₃, 3H).

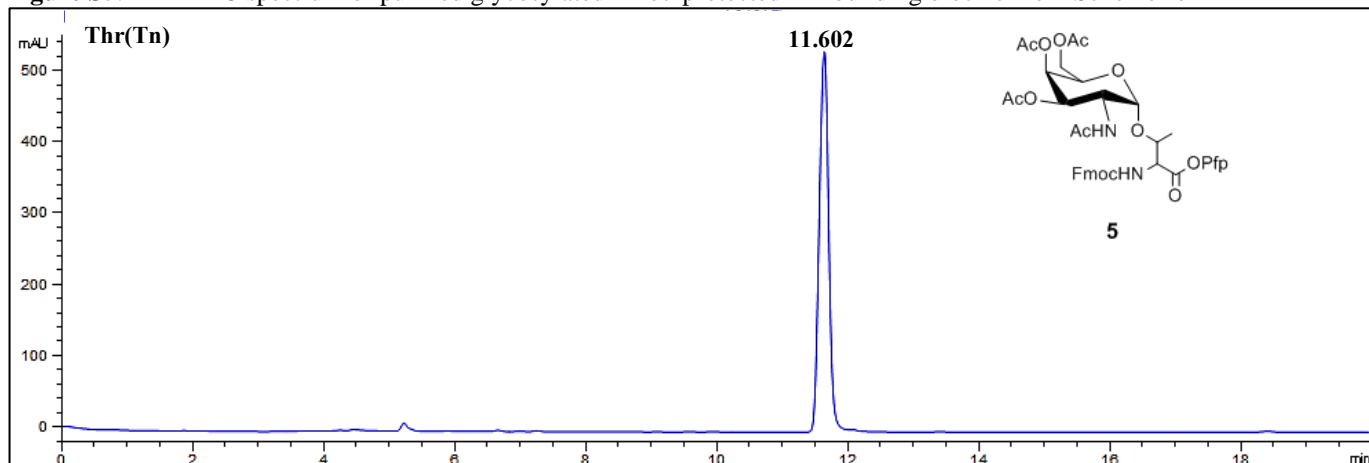
Figure S4. ^{13}C NMR spectrum of purified glycosylated Fmoc-protected Thr building block **4** from Scheme 1.



^{13}C NMR (400 MHz, CDCl_3): δ [ppm] = 170.43, 170.06, 169.94, 166.69, 156.57, 143.59, 141.28, 127.76, 127.10, 125.12, 120.00, 99.19 (C₁ GalNAc), 68.49, 67.82, 67.36, 67.23, 61.79, 58.48, 57.92, 47.03, 20.62, 18.91.

Thr(Tn)

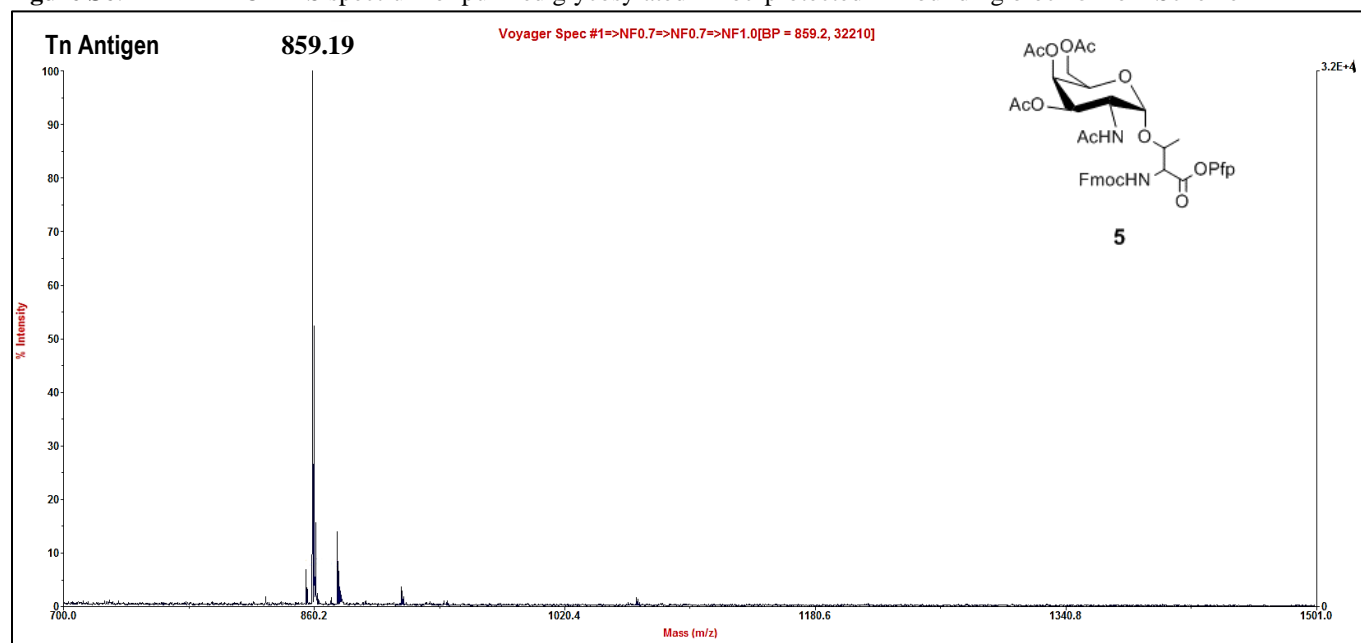
Figure S5. RP-HPLC spectrum of purified glycosylated Fmoc-protected Thr building block **5** from Scheme 1.



HPLC analysis of purified glycosylated Fmoc-protected Thr building block **5** derived from Scheme 1.

Eluents were 0.1% TFA in water (A) and 0.1% TFA in acetonitrile (B). The elution gradient was 40-100% B in 20 mins with a flow rate of 1.0 mL/min. Detection was at wavelength = 214 nm. Retention time (min) = 11.602.

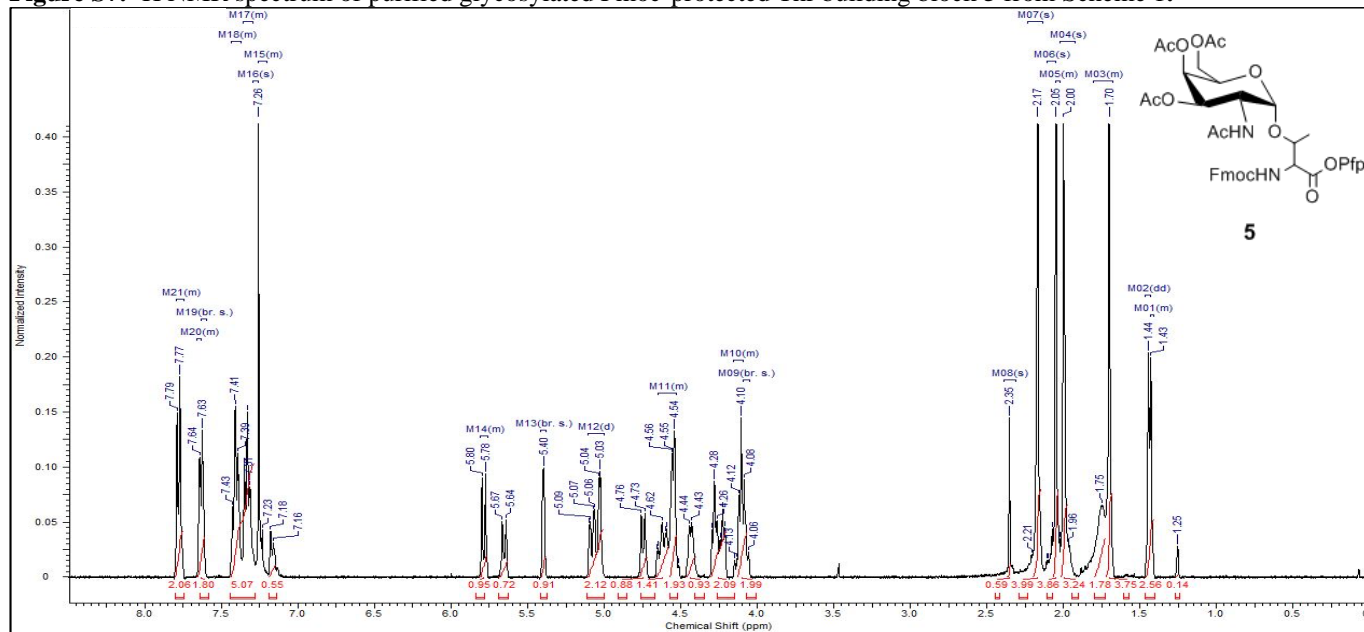
Figure S6. MALDI-TOF MS spectrum of purified glycosylated Fmoc-protected Thr building block **5** from Scheme 1.



MALDI-TOF MS analysis of purified glycosylated Fmoc-protected Thr building block **5** derived from Scheme 1.

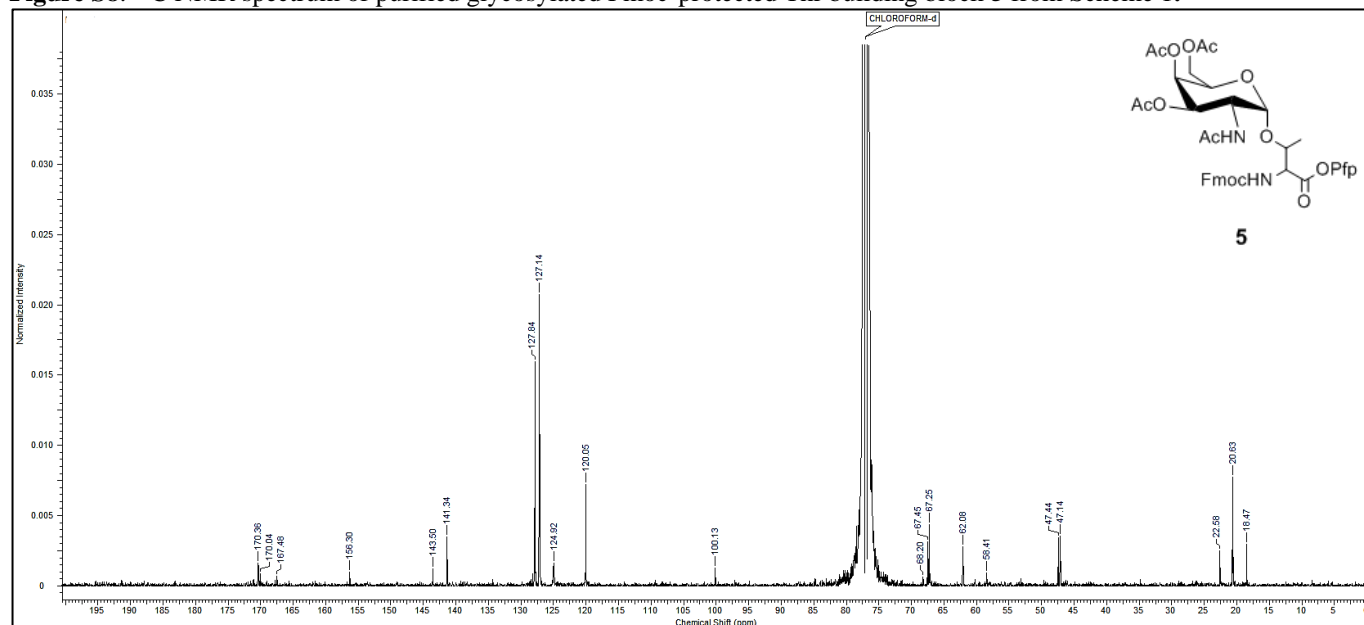
Thr(T_N): [M + Na]⁺ = 859.19 Da (expected, 859.72 Da).

Figure S7. ^1H NMR spectrum of purified glycosylated Fmoc-protected Thr building block **5** from Scheme 1.



^1H NMR (400 MHz, CDCl_3): δ [ppm] = 7.80-7.77 (d, J = 7.4 Hz, Ar-H Fmoc, 2H), 7.64-7.63 (d, J = 7.8 Hz, Ar-H Fmoc, 2H), 7.43-7.39 (m, J = 7.2 Hz, Ar-H Fmoc, 2H), 7.36-7.32 (m, J = 7.3 Hz, Ar-H Fmoc, 2H), 7.18-7.16 (m, NHCOCH_3 , 1H), 5.80-5.78 (d, J = 9.2 Hz, NH-Thr, 1H), 5.67-5.64 (d, J = 10.4 Hz, Gal-H₁, 1H), 5.40 (s, Gal-H₄, 1H), 5.09-5.03 (m, Gal-H₃, 1H), 4.76-4.73 (d, J = 8.2 Hz, αCH Thr, 1H), 4.66-4.54 (m, Gal-H₅, Fmoc CH₂, and βCH Thr, 4H), 4.44-4.43 (m, Gal-H₂, 1H), 4.31-4.22 (m, Fmoc-CH, 1H), 4.13-4.06 (m, Gal-H_{6a-6b}, 2H), 2.17 (s, COCH_3 , 3H), 2.05 (s, COCH_3 , 3H), 2.00 (s, COCH_3 , 3H), 1.70 (s, NHCOCH_3 , 3H), 1.44-1.43 (d, Thr-CH₃, 3H).

Figure S8. ^{13}C NMR spectrum of purified glycosylated Fmoc-protected Thr building block **5** from Scheme 1.



^{13}C NMR (400 MHz, CDCl_3): δ [ppm] = 170.36, 170.04, 167.48, 156.30, 143.50, 141.34, 127.84, 127.14, 124.92, 120.05, 100.13 (C₁ GalNAc), 68.20, 67.45, 67.25, 62.08, 58.41, 47.44, 47.14, 22.58, 20.64, 20.63, 20.62, 18.47.

Peptide Synthesis

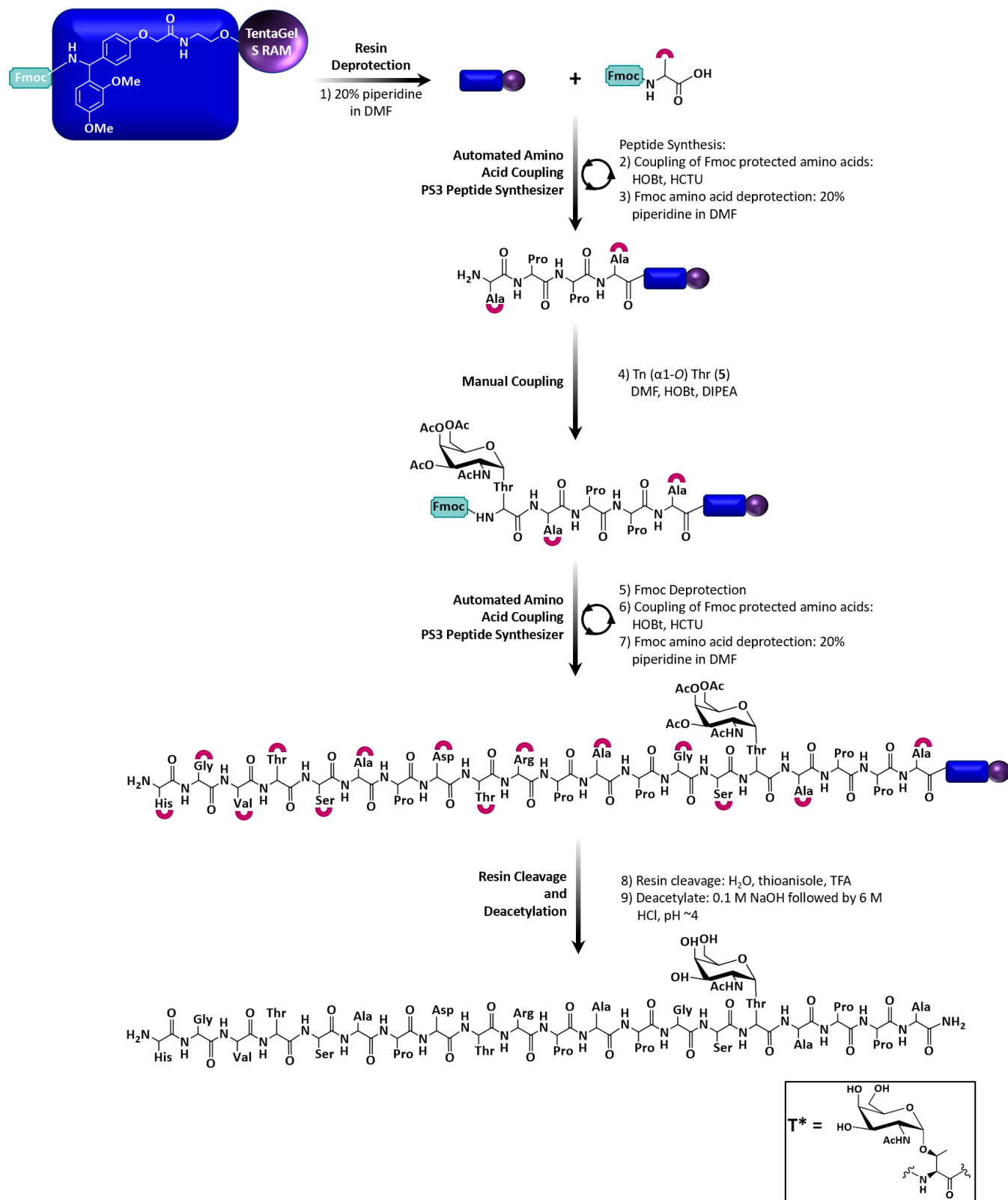
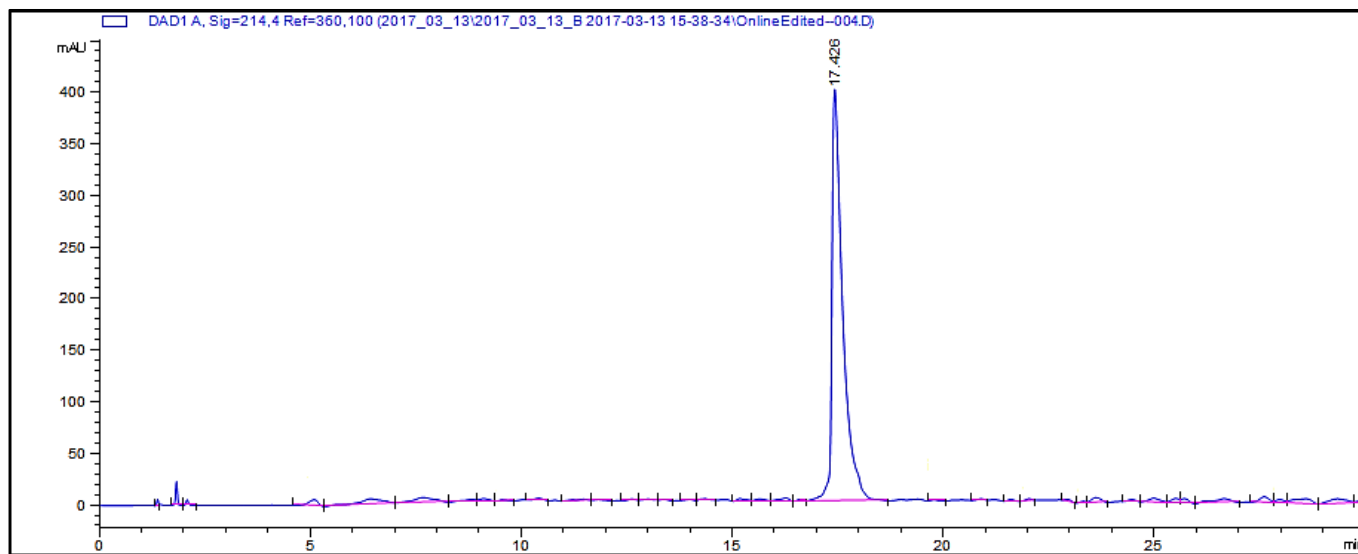


Figure S9. General synthetic scheme for glycopeptides (specifically peptide 7, MUC1: HGVT* Tn SAPDTRPAGSTAPPA).

MUC1

Figure S10. RP-HPLC spectrum of purified MUC1 peptide (6).

MUC1: HGVTSAPDTRPAPGSTAPPA

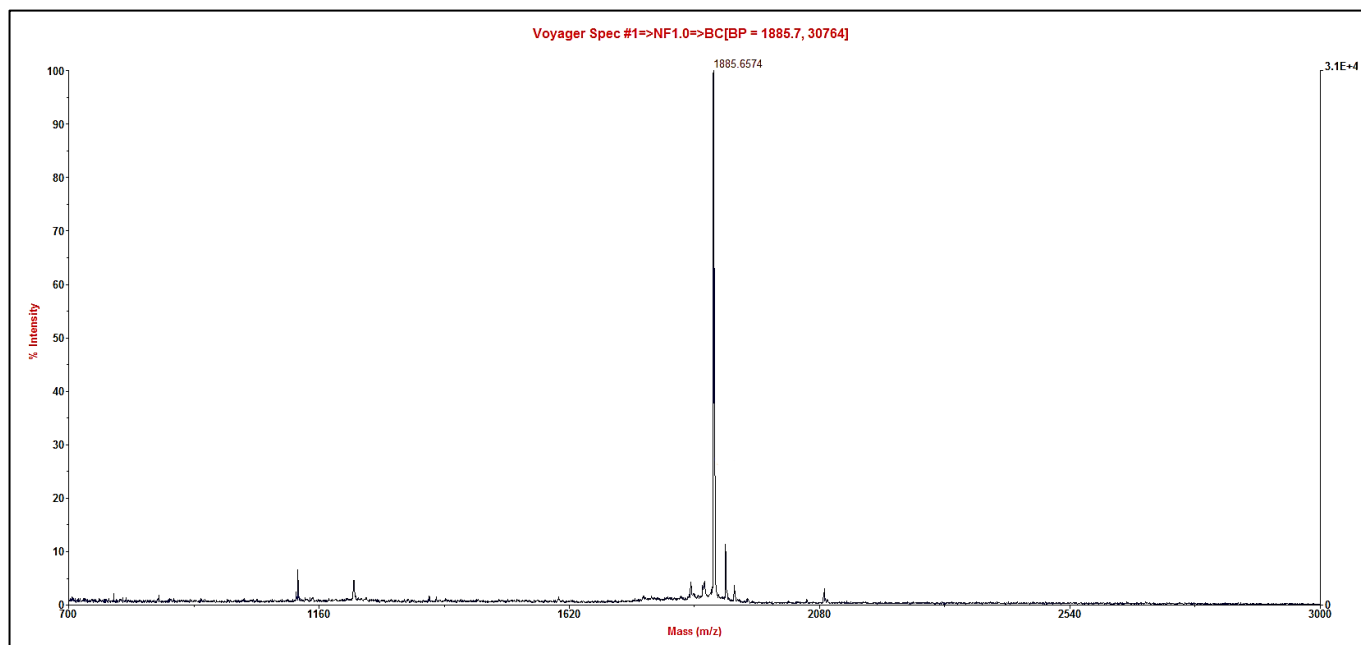


HPLC analysis of purified MUC1 peptide (6).

Eluents were 0.1% TFA in water (A) and 0.1% TFA in acetonitrile (B). The elution gradient was 0-30% B in 30 mins with a flow rate of 1.0 mL/min. Detection was at wavelength = 214 nm. Retention time (min) = 17.42.

Figure S11. MALDI-TOF MS spectrum of purified MUC1 peptide (6).

MUC1: HGVTSAPDTRPAPGSTAPPA



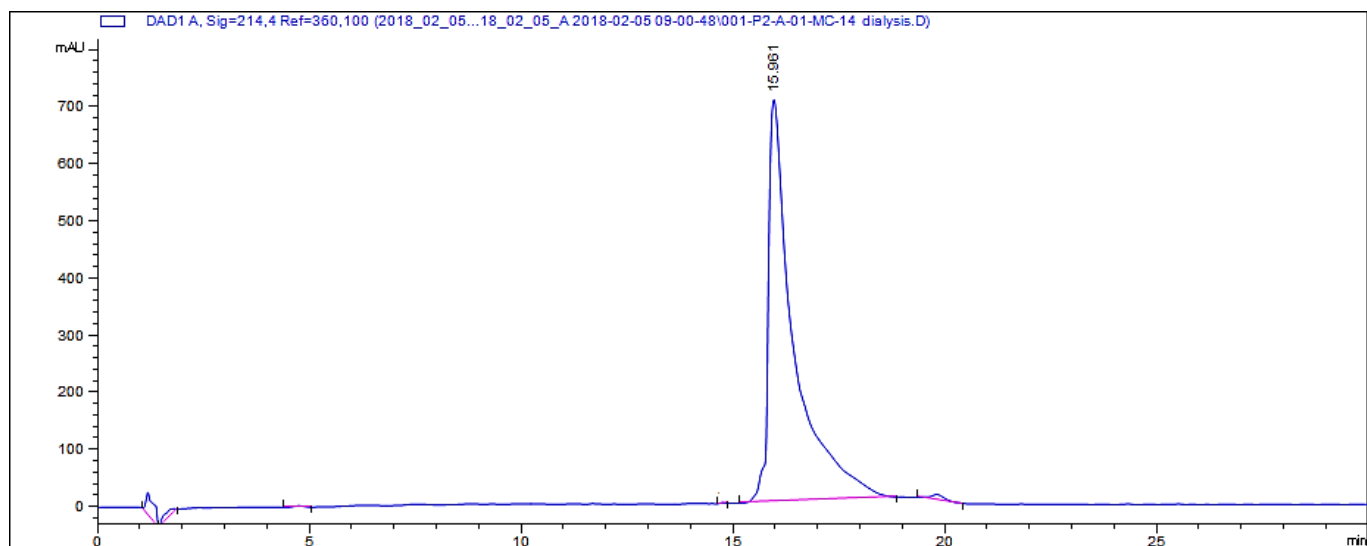
MALDI-TOF MS analysis of purified MUC1 peptide (6).

$[M + H]^+ = 1885.65$ Da (expected, 1884.93 Da).

MUC1-Thr4

Figure S12. RP-HPLC spectrum of purified MUC1-Thr4 peptide (7).

MUC1: HGVT*SAPDTRPAPGSTAPPA



HPLC analysis of purified glycosylated MUC1-Thr4 peptide (7).

Eluents were 0.1% TFA in water (A) and 0.1% TFA in acetonitrile (B). The elution gradient was 0-30% B in 30 mins with a flow rate of 1.0 mL/min. Detection was at wavelength = 214 nm. Retention time (min) = 15.96.

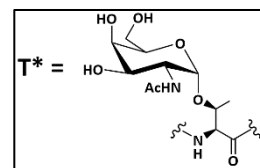
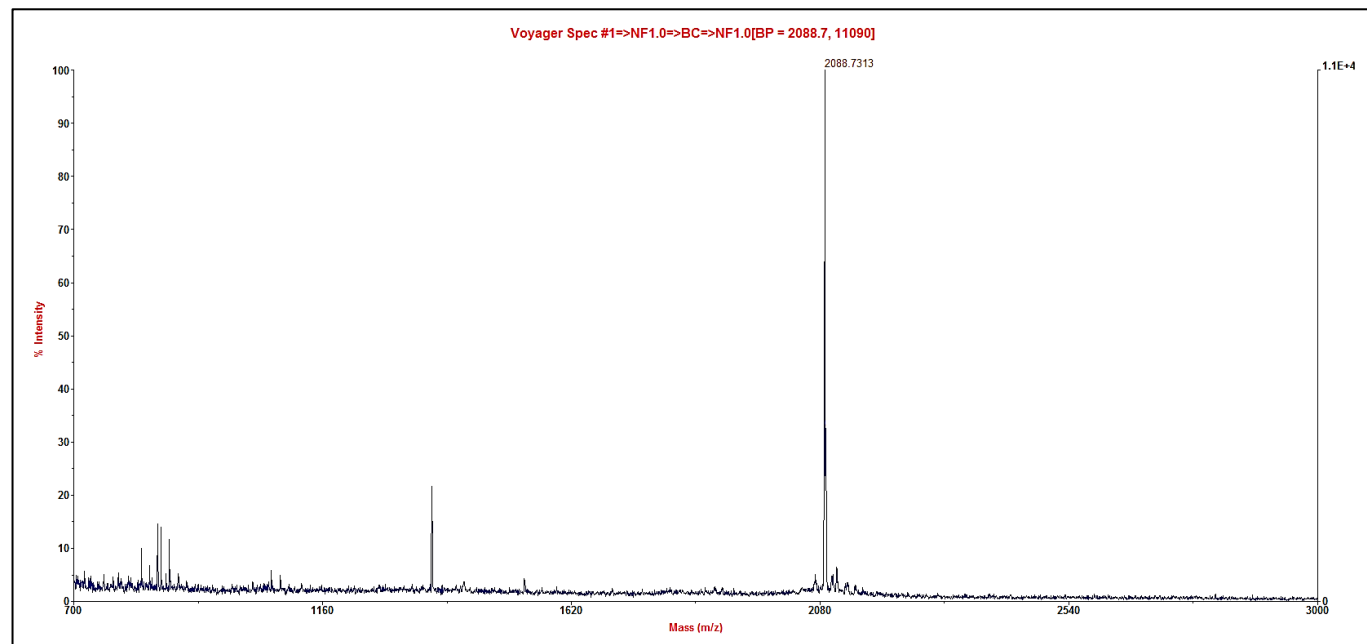


Figure S13. MALDI-TOF MS spectrum of purified MUC1-Thr4 peptide (7).

MUC1: HGVT*SAPDTRPAPGSTAPPA



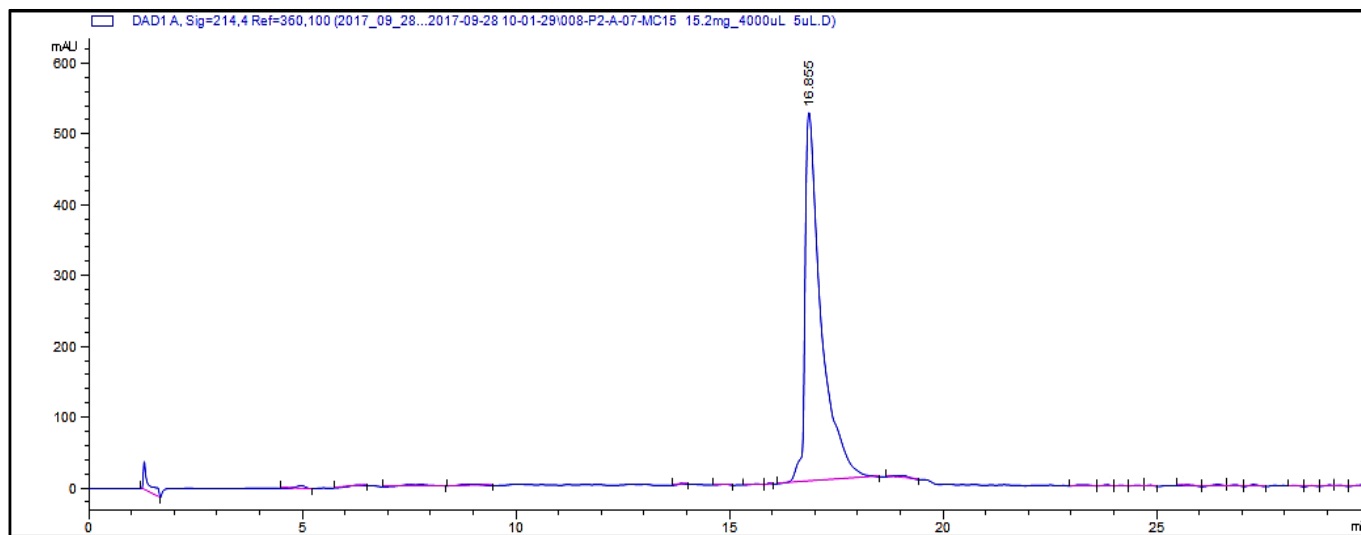
MALDI-TOF MS analysis of purified glycosylated MUC1-Thr4 peptide (7).

$[M + H]^+ = 2088.73$ Da (expected, 2089.25 Da).

MUC1-Thr9

Figure S14. RP-HPLC spectrum of purified MUC1-Thr9 peptide (**8**).

MUC1: HGVTSAPDT*RPAPGSTAPPA



HPLC analysis of purified glycosylated MUC1-Thr9 peptide (**8**).

Eluents were 0.1% TFA in water (A) and 0.1% TFA in acetonitrile (B). The elution gradient was 0-30% B in 30 mins with a flow rate of 1.0 mL/min. Detection was at wavelength = 214 nm. Retention time (min) = 16.85.

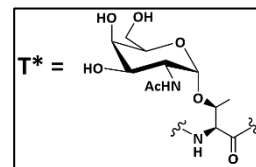
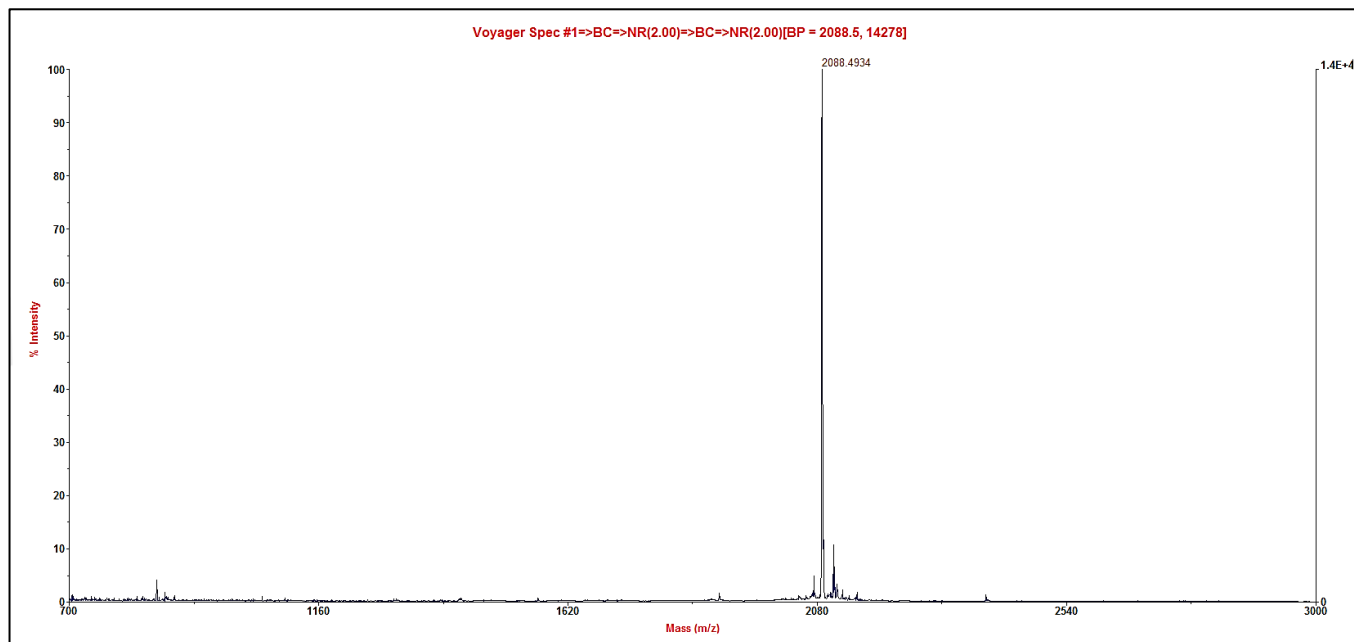


Figure S15. MALDI-TOF MS spectrum of purified MUC1-Thr9 peptide (**8**).

MUC1: HGVTSAPDT*RPAPGSTAPPA

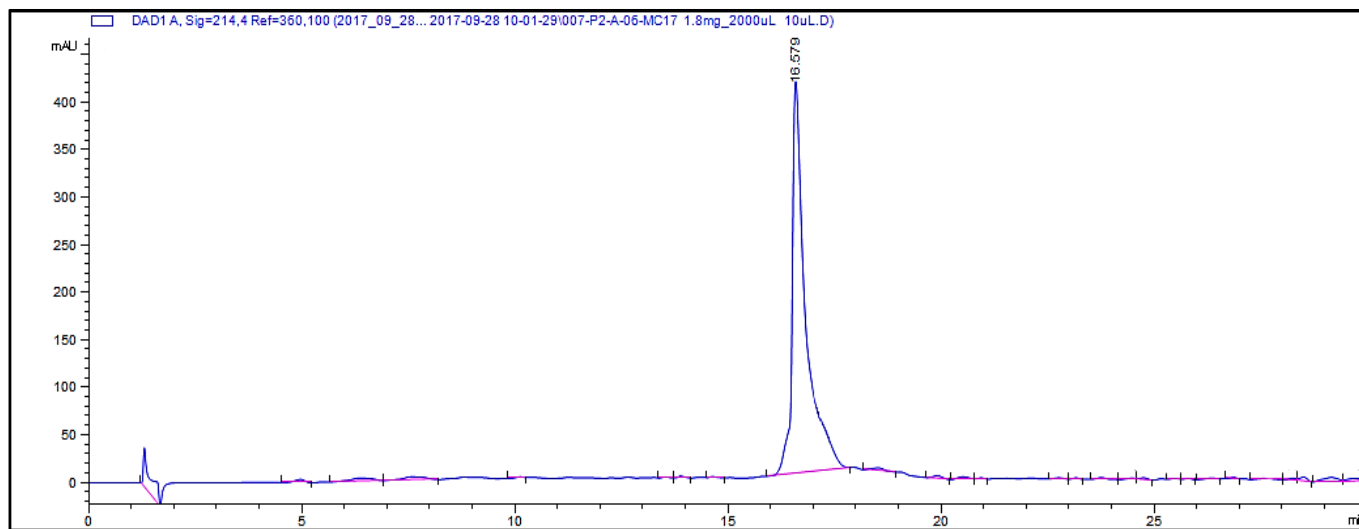


MALDI-TOF MS analysis of purified glycosylated MUC1-Thr9 peptide (**8**).

$[M + H]^+ = 2088.49$ Da (expected, 2089.25 Da).

MUC1-Thr16

Figure S16. RP-HPLC spectrum of purified MUC1-Thr16 peptide (9).
MUC1: HGVTSAPDTRPAPGST*APPA



HPLC analysis of purified glycosylated MUC1-Thr16 peptide (9).

Eluents were 0.1% TFA in water (A) and 0.1% TFA in acetonitrile (B). The elution gradient was 0-30% B in 30 mins with a flow rate of 1.0 mL/min. Detection was at wavelength = 214 nm. Retention time (min) = 16.57.

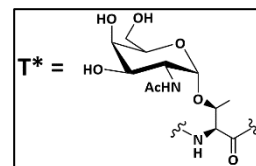
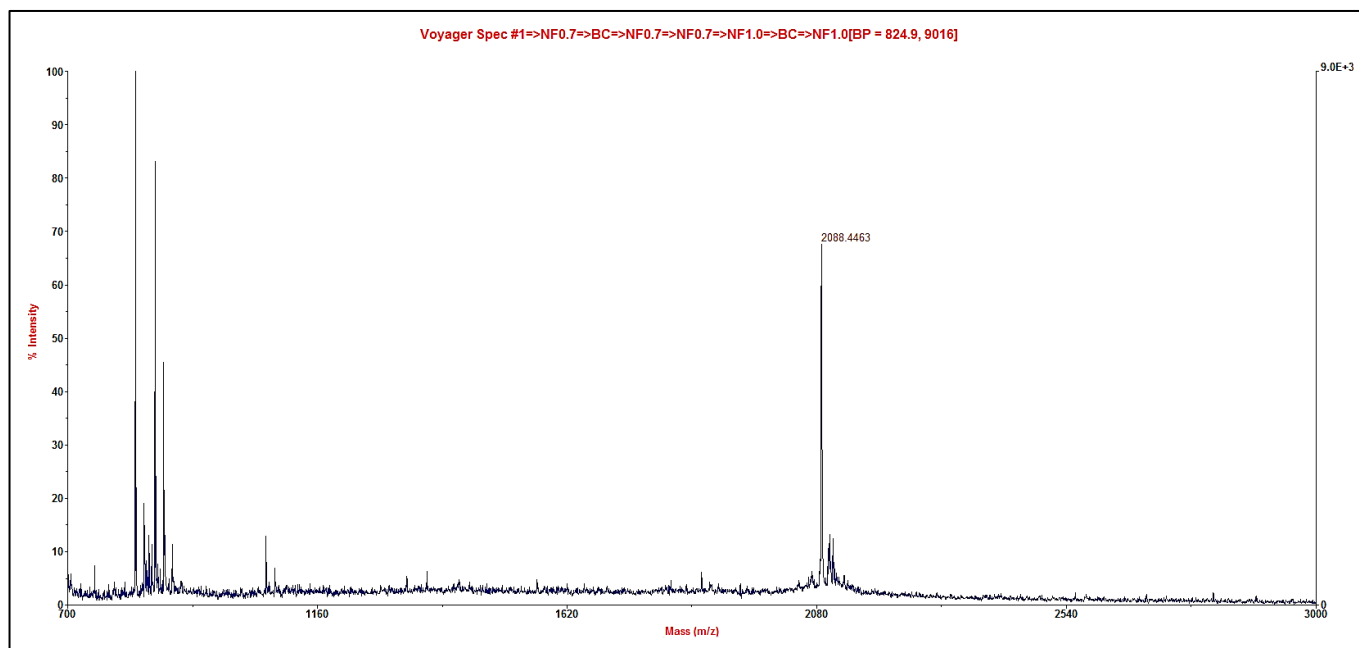


Figure S17. MALDI-TOF MS spectrum of purified MUC1-Thr16 peptide (9).
MUC1: HGVTSAPDTRPAPGST*APPA

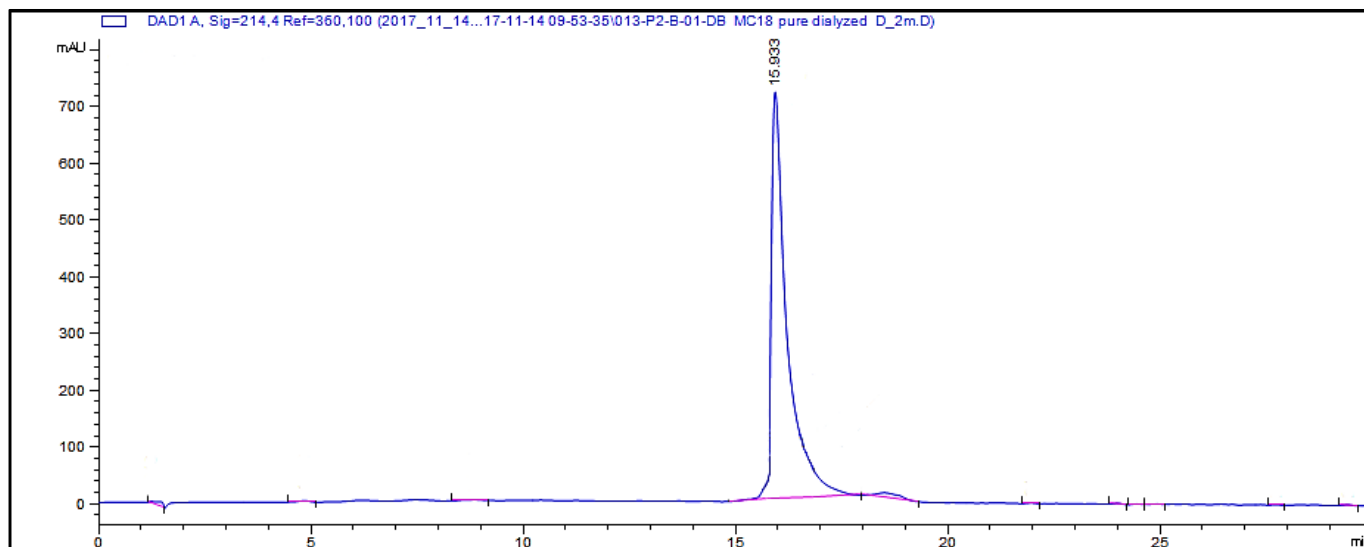


MALDI-TOF MS analysis of purified glycosylated MUC1-Thr16 peptide (9).
[M + H]⁺ = 2088.44 Da (expected, 2089.25 Da).

MUC1-Thr9,16

Figure S18. RP-HPLC spectrum of purified MUC1-Thr9,16 peptide (**10**).

MUC1: HGVTSAPDT*RPAPGST*APPA



HPLC analysis of purified glycosylated MUC1-Thr9,16 peptide (**10**).

Eluents were 0.1% TFA in water (A) and 0.1% TFA in acetonitrile (B). The elution gradient was 0-30% B in 30 mins with a flow rate of 1.0 mL/min. Detection was at wavelength = 214 nm. Retention time (min) = 15.93.

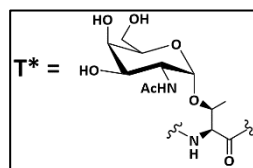
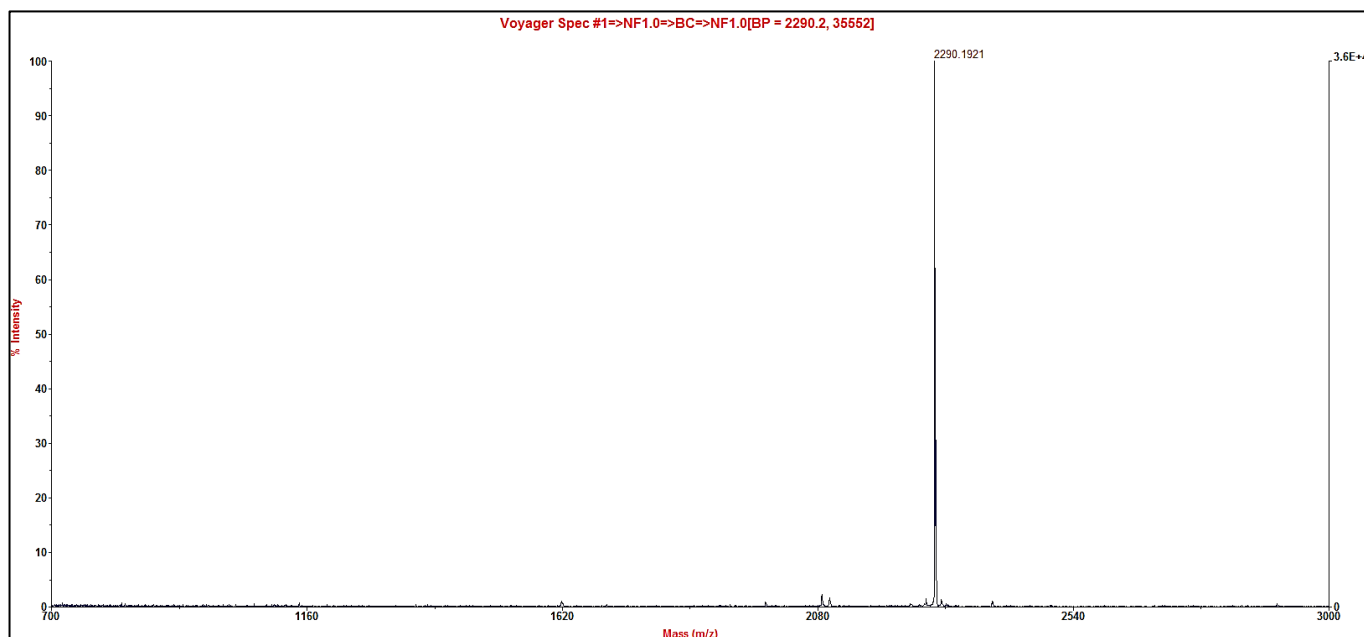


Figure S19. MALDI-TOF MS spectrum of purified MUC1-Thr9,16 peptide (**10**).

MUC1: HGVTSAPDT*RPAPGST*APPA



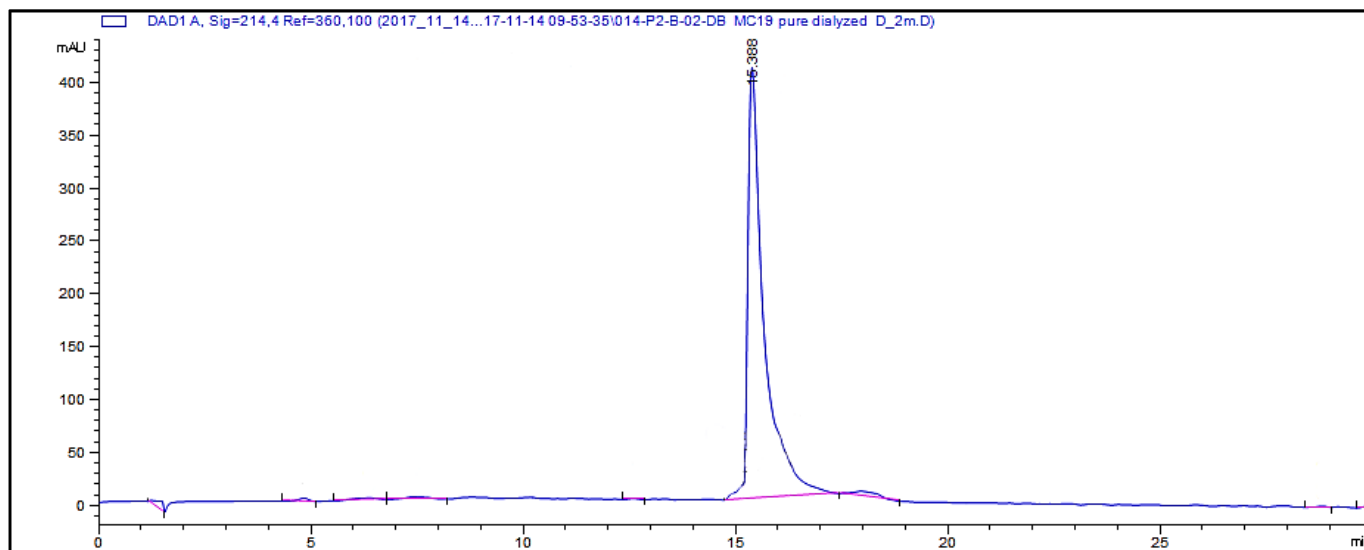
MALDI-TOF MS analysis of purified glycosylated MUC1-Thr9,16 peptide (**10**).

$[M + H]^+ = 2290.19$ Da (expected, 2292.45 Da).

MUC1-Thr4,16

Figure S20. RP-HPLC spectrum of purified MUC1-Thr4,16 peptide (**11**).

MUC1: HGVT*SAPDTRPAGST*APPA



HPLC analysis of purified glycosylated MUC1-Thr4,16 peptide (**11**). Eluents were 0.1% TFA in water (A) and 0.1% TFA in acetonitrile (B). The elution gradient was 0-30% B in 30 mins with a flow rate of 1.0 mL/min. Detection was at wavelength = 214 nm. Retention time (min) = 15.38.

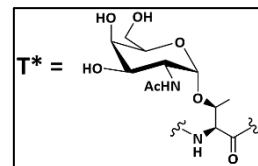
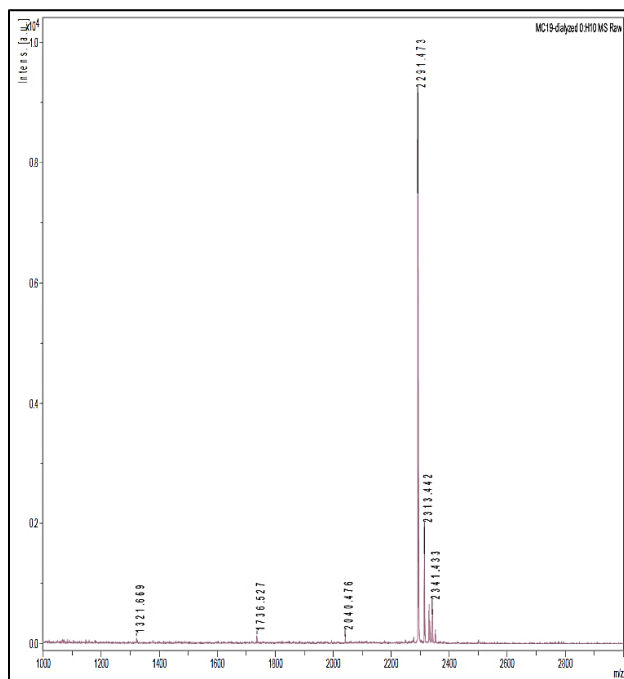


Figure S21. MALDI-TOF MS spectrum of purified MUC1-Thr4,16 peptide (**11**).

MUC1: HGVT*SAPDTRPAGST*APPA

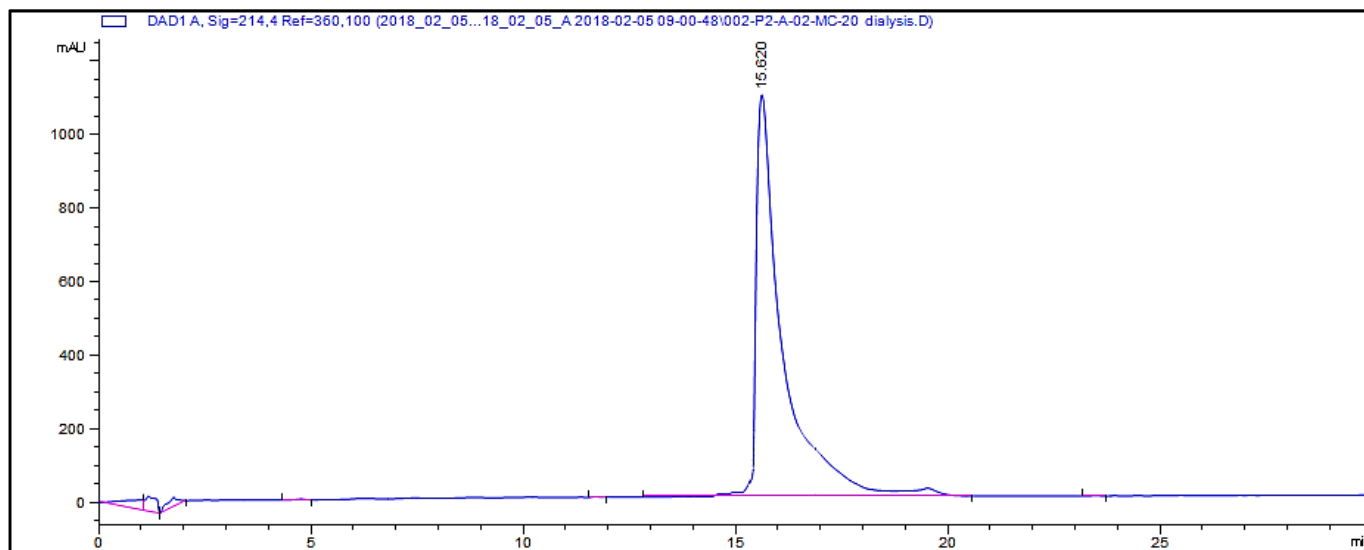


MALDI-TOF MS analysis of purified glycosylated MUC1-Thr4,16 peptide (**11**) was performed with a MicroFlex LT system (Bruker). $[M + H]^+ = 2291.47$ Da (expected, 2292.45 Da).

MUC1-Thr4,9

Figure S22. RP-HPLC spectrum of purified MUC1-Thr4,9 peptide (**12**).

MUC1: HGVT*SAPDT*RPAPGSTAPPA



HPLC analysis of purified glycosylated MUC1-Thr4,9 peptide (**12**).

Eluents were 0.1% TFA in water (A) and 0.1% TFA in acetonitrile (B). The elution gradient was 0-30% B in 30 mins with a flow rate of 1.0 mL/min. Detection was at wavelength = 214 nm. Retention time (min) = 15.62.

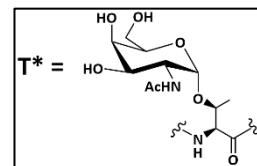
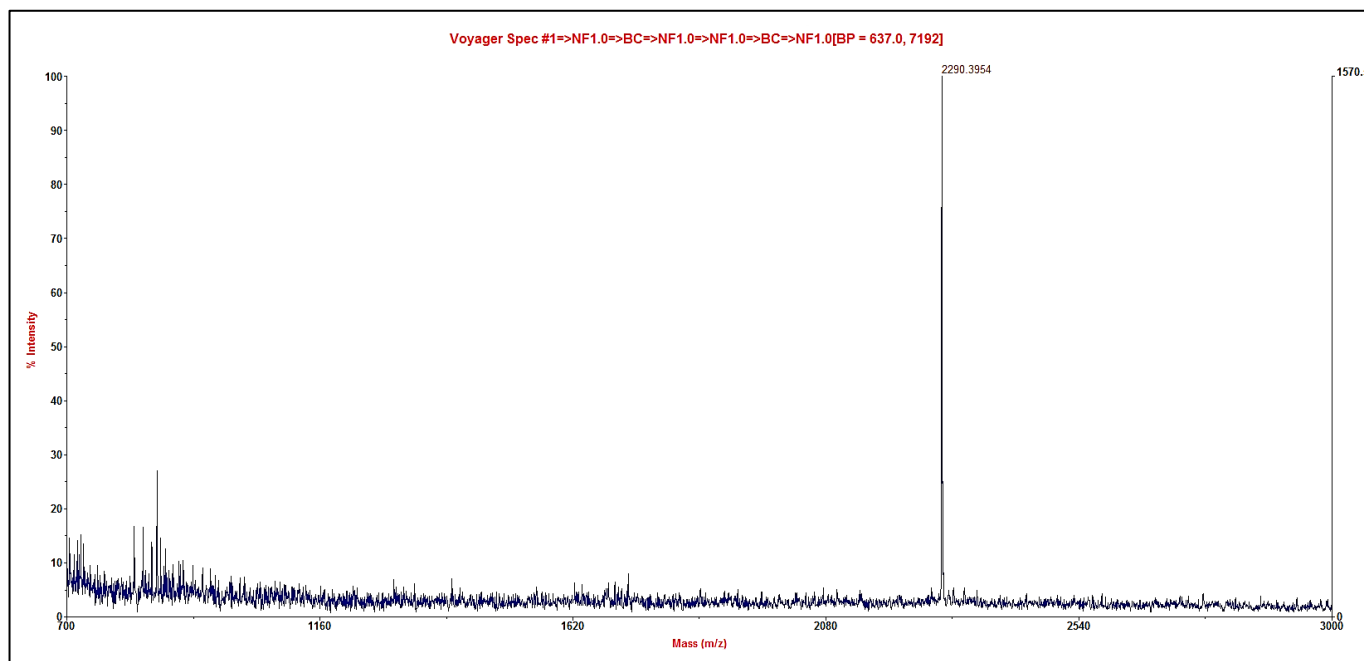


Figure S23. MALDI-TOF MS spectrum of purified MUC1-Thr4,9 peptide (**12**).

MUC1: HGVT*SAPDT*RPAPGSTAPPA



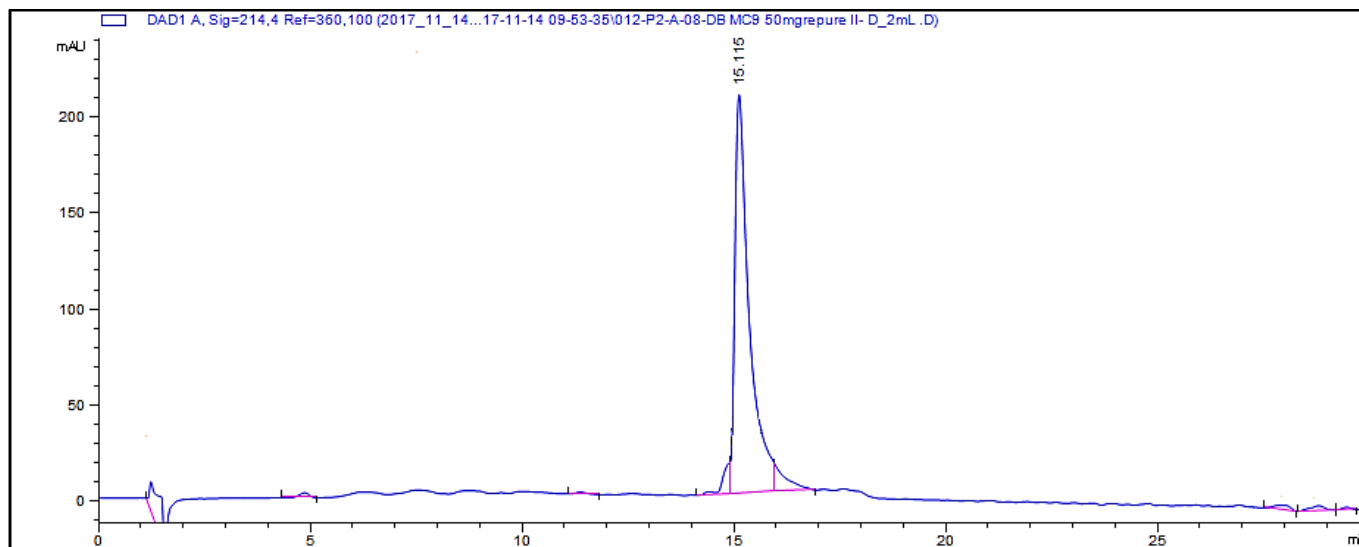
MALDI-TOF MS analysis of purified glycosylated MUC1-Thr4,9 peptide (**12**).

[M + H]⁺ = 2290.39 Da (expected, 2292.45 Da).

MUC1-Thr4,9,16

Figure S24. RP-HPLC spectrum of purified MUC1-Thr4,9,16 peptide (**13**).

MUC1: HGVT*SAPDT*RPAPGST*APPA



HPLC analysis of purified glycosylated MUC1-Thr4,9,16 peptide (**13**).

Eluents were 0.1% TFA in water (A) and 0.1% TFA in acetonitrile (B). The elution gradient was 0-30% B in 30 mins with a flow rate of 1.0 mL/min. Detection was at wavelength = 214 nm. Retention time (min) = 15.11.

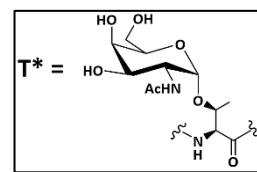
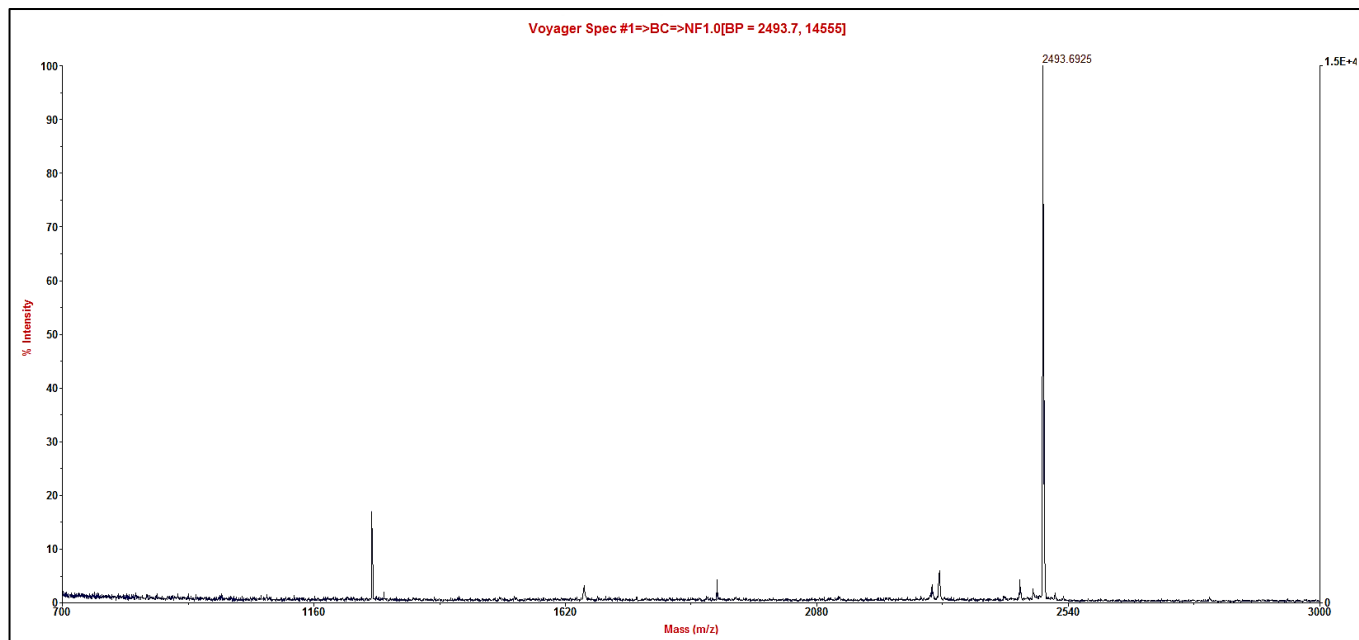


Figure S25. MALDI-TOF MS spectrum of purified MUC1-Thr4,9,16 peptide (**13**).

MUC1: HGVT*SAPDT*RPAPGST*APPA

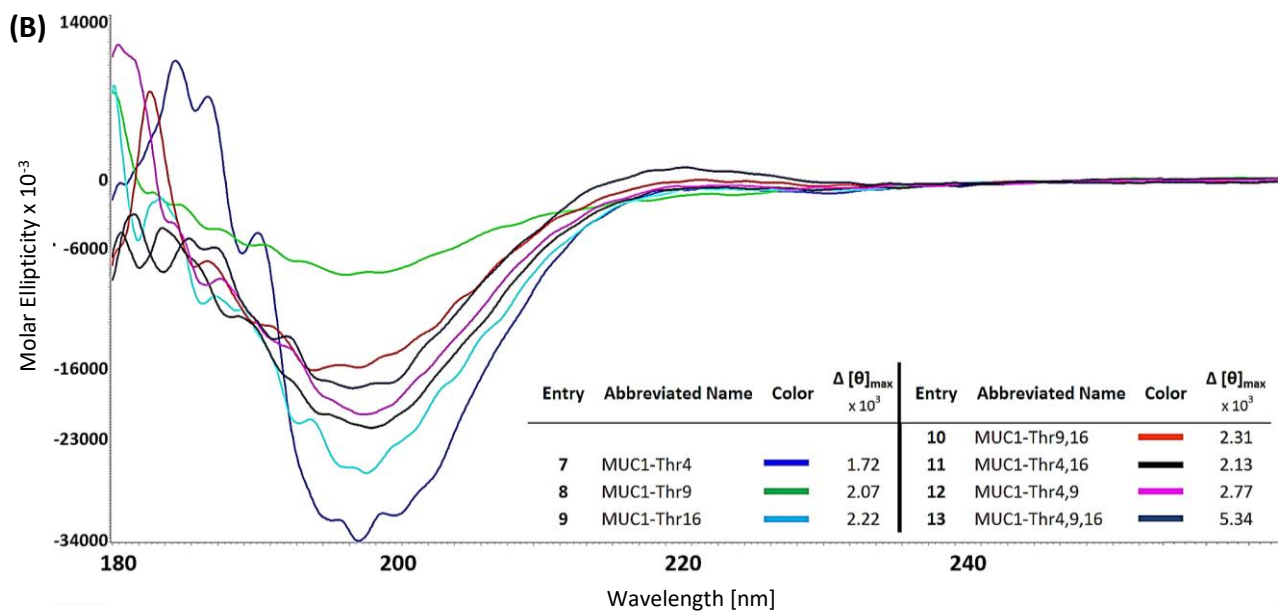
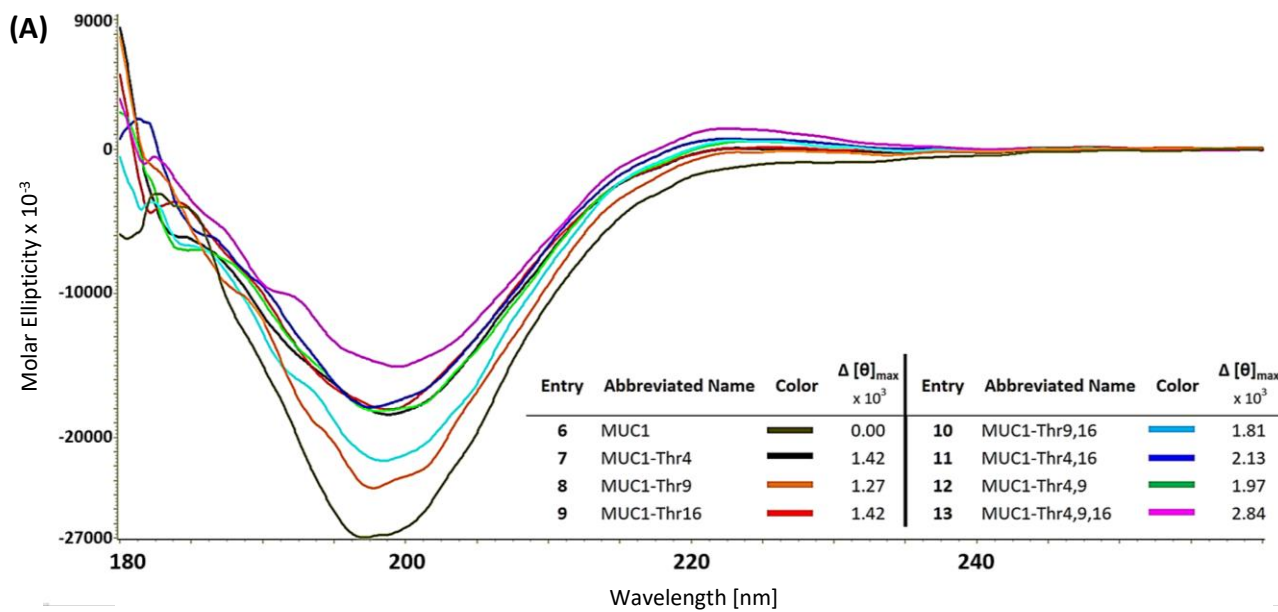


MALDI-TOF MS analysis of purified glycosylated MUC1-Thr4,9,16 peptide (**13**).

$[M + H]^+ = 2493.69$ Da (expected, 2495.28 Da).

Circular Dichroism

Figure S26. Circular dichroism spectra of MUC1 (glyco)peptides in buffered (A) H₂O and (B) D₂O. $\Delta[\theta]_{\max}$ value represents each peptide molar ellipticity normalized against MUC1 $[\theta]_{\max}$ in deg cm² dmol⁻¹.



Macrophage Galactose Lectin

Figure S27A. Molecular mass determination of hMGL by MALDI-TOF MS.

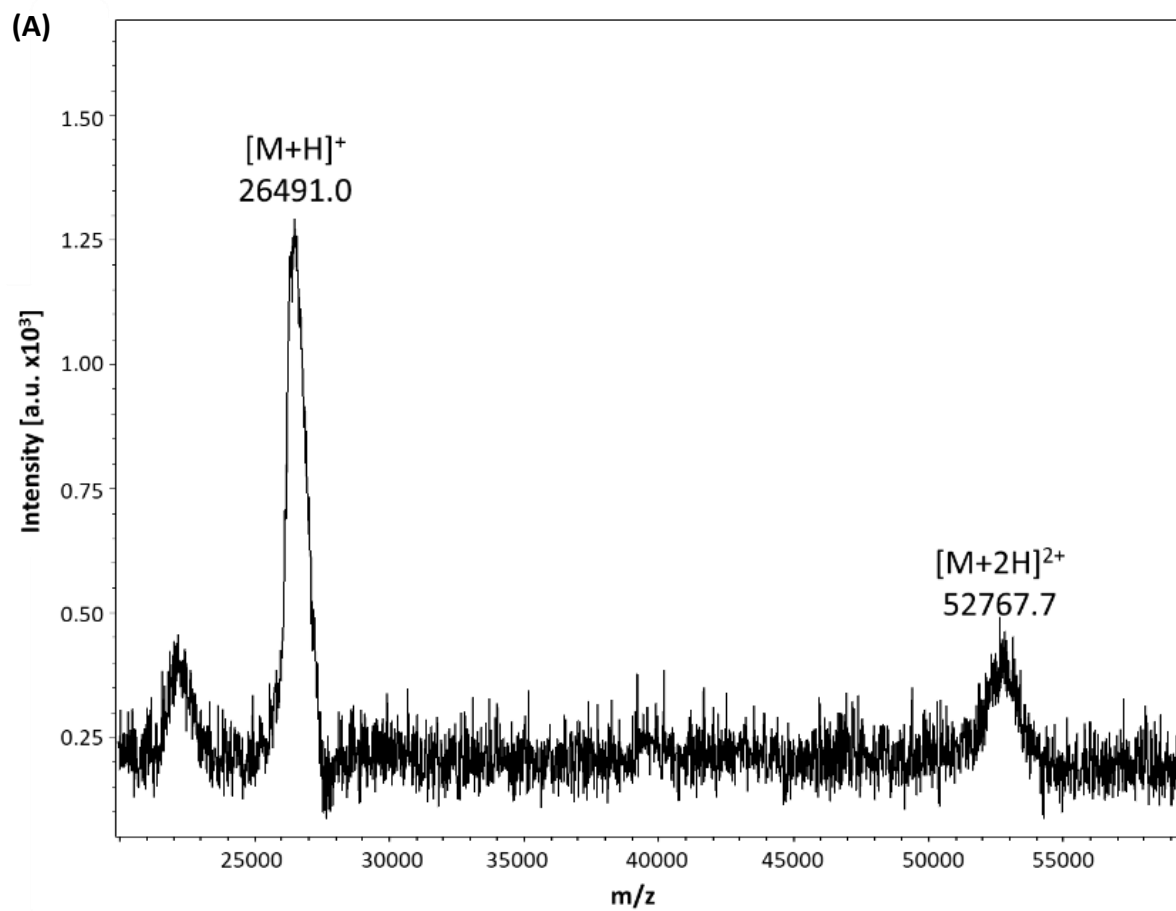
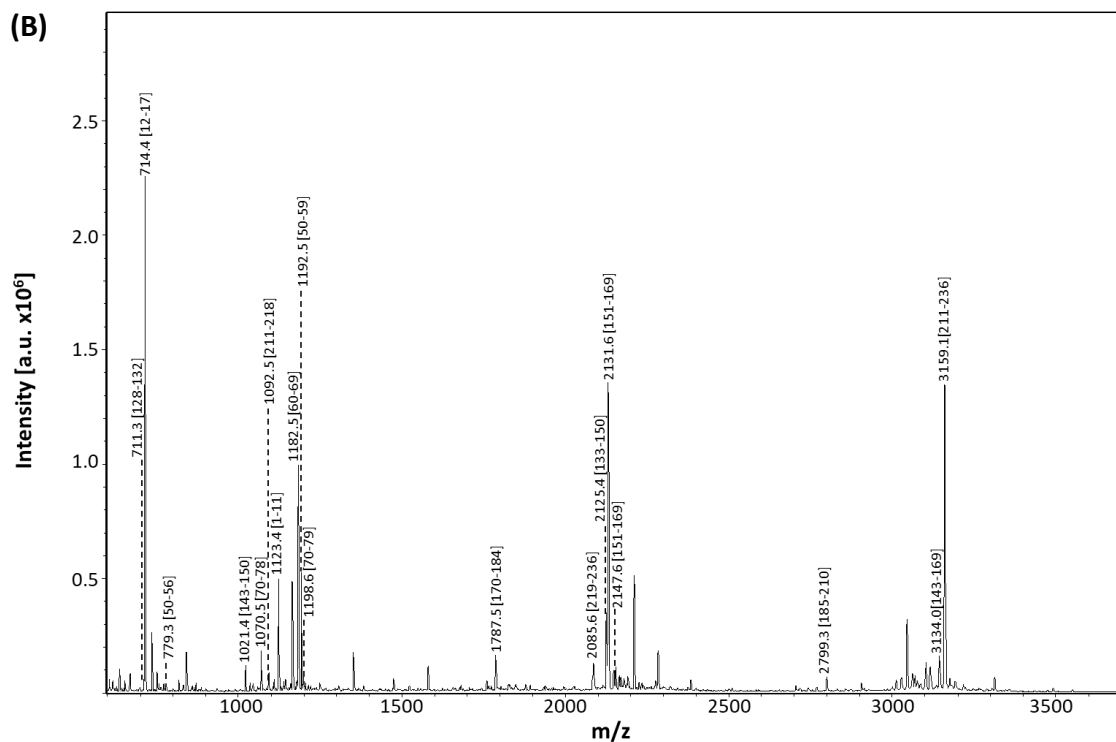


Figure S27B. Tryptic peptide mass fingerprinting of hMGL by MALDI-TOF MS.



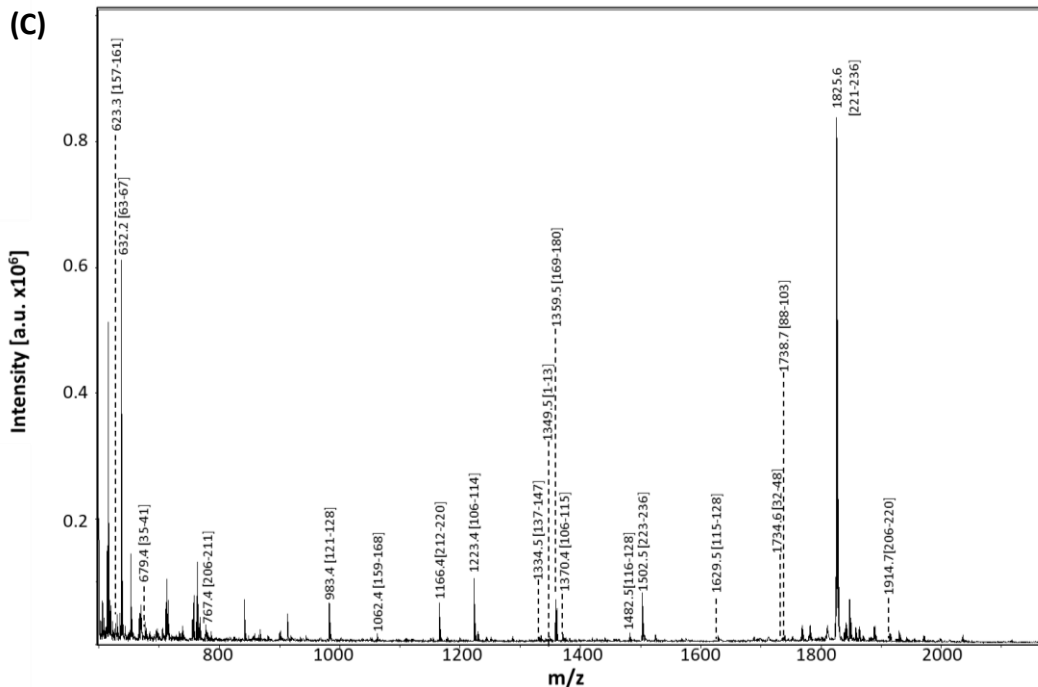
List of detected peptides with their calculated (calc) and experimentally measured (exp) mass values.

Sequence	[MH] ⁺ (mono) calc	[MH] ⁺ (mono) exp
YCQLK ¹	711.3	711.3
ILVTLR	714.5	714.4
AEVEGFK	779.4	779.3
EEQNFVQK	1021.5	1021.4
VQQLVQDLK	1070.6	1070.5
WNDDVCQR ¹	1092.5	1092.5
ASMTGGQQMGR	1123.5	1123.4
ASMTGGQQMGR ^{2,2}	1155.5	1155.4
QAVHSEMLLR	1183.6	1183.5
AEVEGFKQER	1192.6	1192.5
VQQLVQDLKK	1198.7	1198.6
WVDGTDYATGFQNWK	1787.8	1787.5
PYHWVCEAGLQTSQESH ¹	2085.9	2085.6
NAHLVINSREEQNFVQK	2125.1	2125.4
YLGSAYTWGLSDPEGAWK	2132.0	2131.6
YLGSAYTWGLSDPEGAWK ²	2148.0	2147.6
PGQPDDWQGHGLGGGEDCAHFHPDGR ¹	2799.2	2799.3
EEQNFVQKYLGSAYTWGLSDPEGAWK	3134.5	3134.0
WNDDVCQRPYHWVCEAGLQTSQESH ¹	3159.3	3159.1

Sequence coverage (66.1%)

ASMTGGQQMGRILVTLRTDFSNFTSNTVAEIQALTSQGSLEETIASLKAEVEGFKQERQAVHSEMLLRVQQLVQDLK
 KLTCQVATLNNNGEEASTEGTCCPVNWVEHQDSCYWFSHSGMSWAEAEKYCQLKNAHLVINSREEQNFVQKYLGS
 SAYTWGLSDPEGAWKWVDGTDYATGFQNWKPGQPDDWQGHGLGGGEDCAHFHPDGRWNDDVCQRPYHWVCE
 AGLQTSQESH

Figure S27C. Chymotryptic peptide mass fingerprinting of hMGL by MALDI-TOF MS.



List of detected peptides with their calculated (calc) and experimentally measured (exp) mass values.

Sequence	[MH] ⁺ (mono) calc	[MH] ⁺ (mono) exp
TWMGL ²	623.3	623.3
HSEML ²	632.3	632.2
TSQGSSL	679.3	679.4
HPDGRW	767.4	767.4
SWAEAEKY	983.4	983.4
MGLSDPEGAW	1062.5	1062.4
NDDVCQRPY ¹	1166.5	1166.4
VEHQDSCYW ²	1223.5	1223.4
VVINSREEQNF	1334.6	1334.5
ASMTGGQMGRIL	1349.7	1349.5
KWVDGTDYATGF	1359.6	1359.5
VEHQDSCYWF ¹	1370.5	1370.4
SHSGMSWAEAEKY	1482.6	1482.5
VCEAGLGQTSQESH ¹	1502.7	1502.5
FSHSGMSWAEAEKY	1629.7	1629.5
QALTSQGSSLEETIASL	1734.9	1734.6
NNNGEEASTEGTCCPV	1738.7	1738.7
HWVCEAGLGQTSQESH ¹	1825.8	1825.6
HPDGRWNDDVCQRPY ¹	1914.8	1914.7

Sequence Coverage (67.8%)

ASMTGGQMGRILVTLRTDFSNFTSNTVAEIQALTSQGSSLEETIASLKAIEVEGFKQERQAVHSEMLLRVQQLVQDLK
 KLTCQVATLNNNGEEASTEGTCCPVNWEHQDSCYWFHSGMSWAEAEKYCQLKNAHLVVINSREEQNFVQKYL
 SAYTWMGLSDPEGAWKWVDGTDYATGFQNWKPGQPDDWQGHGLGGEDCAHFHPDGRWNDDVCQRPYHWVCE
 AGLGQTSQESH

Figure S27D. Combined sequence coverage of tryptic and chymotryptic peptide mass fingerprinting of hMGL by MALDI-TOF MS.

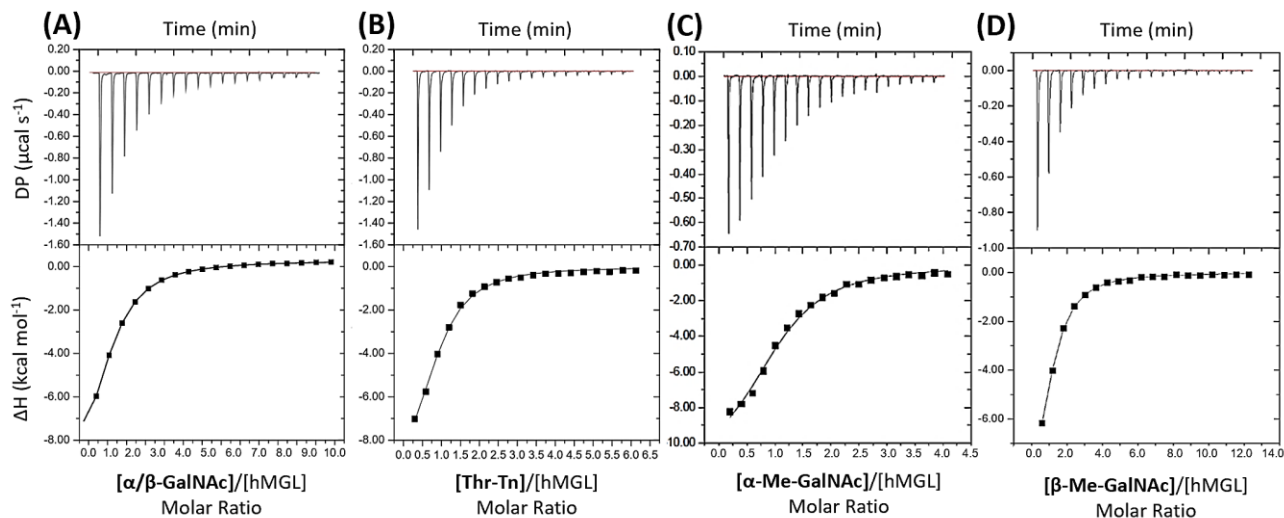
(D)

Sequence coverage (89.4%)

ASMTGGQQMGRILVTLRTDFSNFTSNTVAEIQALTSQGSLEETIASLKAEVEGFKQERQAVHSEMLLRVQQLVQDLK
KLTCQVATLNNNGEEASTEGTCCPVNWVEHQDSCYWFSHSGMSWAEAEKYCQLKNAHLVVINSREEQNFVQKYLG
SAYTWMGLSDPEGAWKWVDGTDYATGFQNWKPGQPDDWQGHGLGGEDCAHFHPDGRWNDDVCQRPYHWVCE
AGLGQTSQESH

Isothermal Titration Calorimetry

Figure S28. ITC binding data for free glycan-MGL interactions. Isotherms corresponding to binding of (A) α/β -GalNAc (1.50 mM) with hMGL (29.6 μ M), (B) Thr-Tn (1.50 mM) with hMGL (50.0 μ M), (C) α -Me-GalNAc (1.50 mM) with hMGL (50.0 μ M), and (D) β -Me-GalNAc (1.50 mM) with hMGL (50.0 μ M). The titrations, integrated data, and signature plots are shown in the upper, middle, and lower panels. The titrations were performed in buffered (10 mM HEPES sodium salt, 50 mM NaCl, and 2 mM CaCl_2 at pH 7.4) H_2O at 25°C.



n	0.99	n	1.02	n	1.03	n	0.97
K_a (10^4 M^{-1})	5.65 ± 0.28	K_a (10^4 M^{-1})	6.17 ± 0.01	K_a (10^4 M^{-1})	12.90 ± 0.40	K_a (10^4 M^{-1})	7.10 ± 0.26
ΔH (kcal/mol)	-11.30 ± 0.13	ΔH (kcal/mol)	-11.08 ± 0.49	ΔH (kcal/mol)	-11.60 ± 0.48	ΔH (kcal/mol)	-11.62 ± 0.45
$-T\Delta S$ (kcal/mol)	4.81	$-T\Delta S$ (kcal/mol)	4.30	$-T\Delta S$ (kcal/mol)	4.65	$-T\Delta S$ (kcal/mol)	5.01
K_d (μM)	17.70 ± 0.28	K_d (μM)	16.20 ± 0.01	K_d (μM)	7.80 ± 0.40	K_d (μM)	14.10 ± 0.26

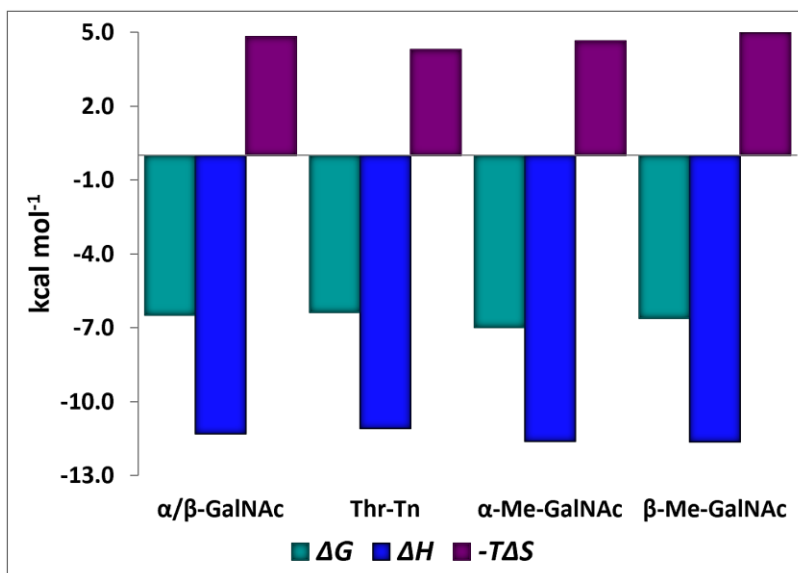


Figure S29. ITC binding data for MUC1 glycopeptide-MGL interactions. Isotherms corresponding to binding of (A) MUC1-Thr4 (0.50 mM) with hMGL (11.5 μ M), (B) MUC1-Thr9 (0.44 mM) with hMGL (19.0 μ M), (C) MUC1-Thr16 (0.50 mM) with hMGL (22.0 μ M), (D) MUC1-Thr9,16 (0.50 mM) with hMGL (19.0 μ M), (E) MUC1-Thr4,16 (0.50 mM) with hMGL (20.0 μ M), (F) MUC1-Thr4,9 (0.50 mM) with hMGL (11.0 μ M), and (G) MUC1-Thr4,9,16 (0.25 mM) with hMGL (20.0 μ M). The titrations, integrated data, and signature plots are shown in the upper, middle, and lower panels. The titrations were performed in buffered (10 mM HEPES sodium salt, 50 mM NaCl, and 2 mM CaCl₂ at pH 7.4) H₂O at 25°C.

MUC1-Thr4: HGVT*SAPDTRPAPGSTAPPA

MUC1-Thr9,16: HGVTAPDT*RPAPGST*APPA

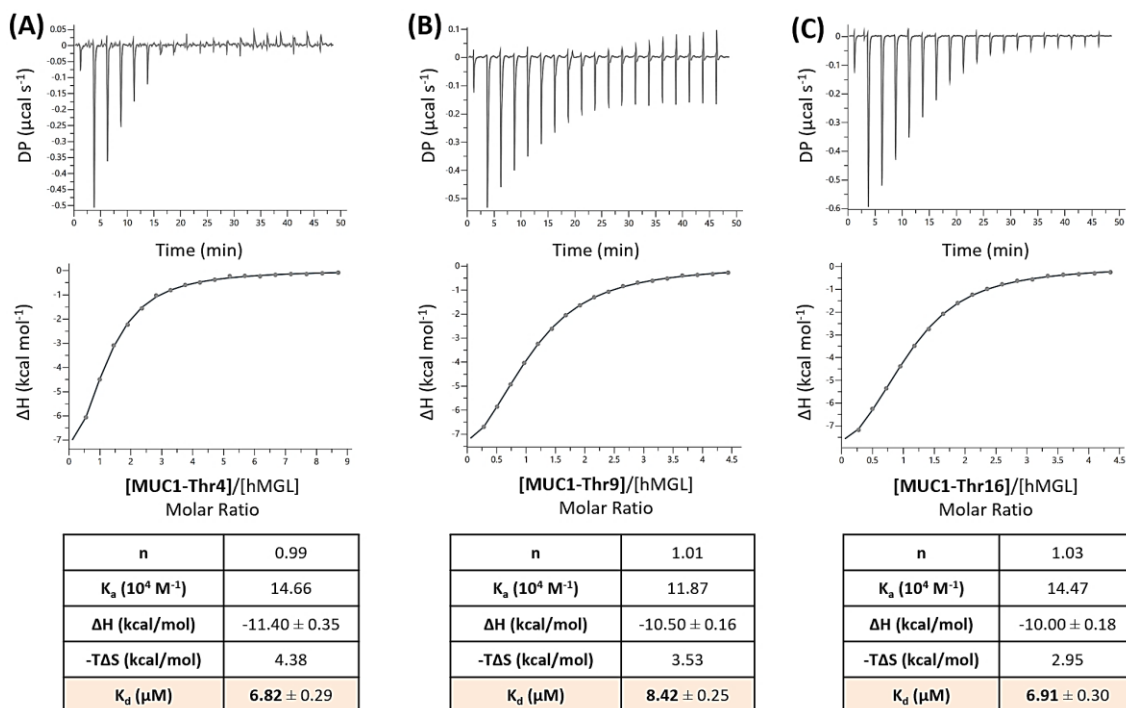
MUC1-Thr9: HGVTAPDT*RPAPGSTAPPA

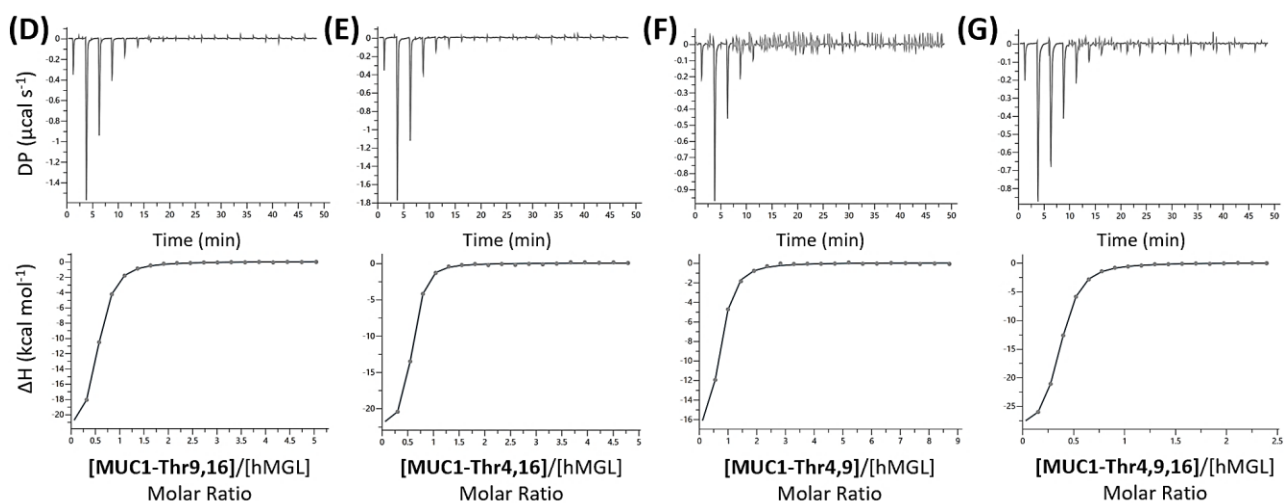
MUC1-Thr4,16: HGVT*SAPDTRPAPGST*APPA

MUC1-Thr16: HGVTAPDTRPAPGST*APPA

MUC1-Thr4,9: HGVT*SAPDT*RPAPGSTAPPA

MUC1-Thr4,9,16: HGVT*SAPDT*RPAPGST*APPA





n	0.46
K_a (10^4 M $^{-1}$)	81.30
ΔH (kcal/mol)	-24.00 ± 0.16
$-T\Delta S$ (kcal/mol)	16.00
K_d (μ M)	1.23 ± 0.02

n	0.48
K_a (10^4 M $^{-1}$)	144.92
ΔH (kcal/mol)	-22.80 ± 0.20
$-T\Delta S$ (kcal/mol)	14.30
K_d (μ M)	0.69 ± 0.02

n	0.50
K_a (10^4 M $^{-1}$)	70.92
ΔH (kcal/mol)	-20.70 ± 1.12
$-T\Delta S$ (kcal/mol)	12.70
K_d (μ M)	1.41 ± 0.13

n	0.32
K_a (10^4 M $^{-1}$)	166.67
ΔH (kcal/mol)	-30.30 ± 0.11
$-T\Delta S$ (kcal/mol)	21.80
K_d (μ M)	0.60 ± 0.01

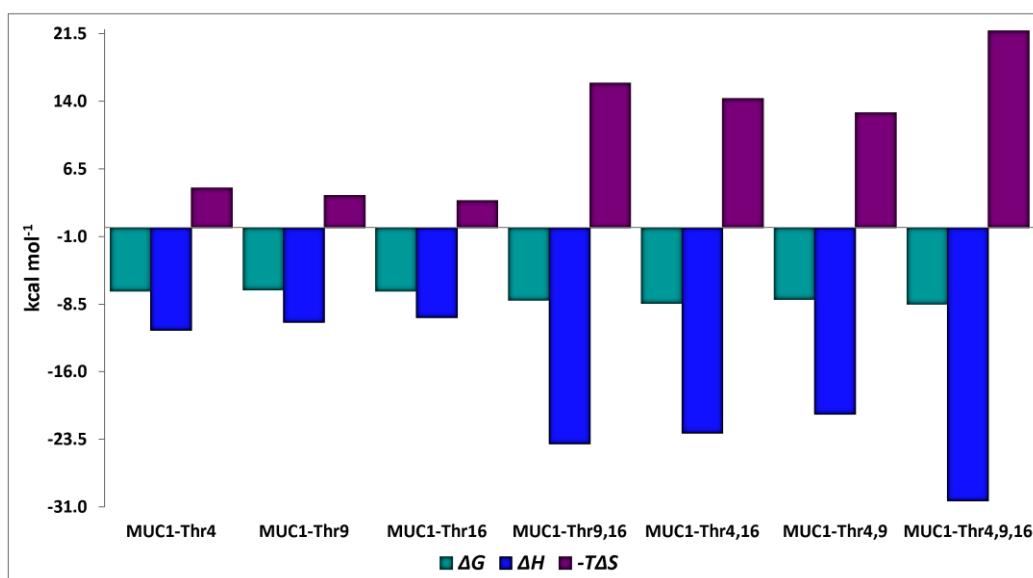


Figure S30. Thermodynamics of free GalNAc and MUC1 glycopeptide-hMGL interactions. Isotherms corresponding to binding of (A) α/β -GalNAc (1.50 mM) with hMGL (28.6 μ M), (B) MUC1-Thr4 (0.50 mM) with hMGL (21.0 μ M), (C) MUC1-Thr9 (0.50 mM) with hMGL (17.5 μ M), (D) MUC1-Thr16 (0.50 mM) with hMGL (14.4 μ M), (E) MUC1-Thr9,16 (0.50 mM) with hMGL (20.0 μ M), (F) MUC1-Thr4,16 (0.50 mM) with hMGL (19.0 μ M), (G) MUC1-Thr4,9 (0.50 mM) with hMGL (24.5 μ M), and (H) MUC1-Thr4,9,16 (0.25 mM) with hMGL (21.0 μ M). The titrations, integrated data, and signature plots are shown in the upper, middle, and lower panels. The titrations were performed in buffered (10 mM HEPES sodium salt, 50 mM NaCl, and 2 mM CaCl_2 at pH 7.4) D_2O at 25 $^\circ\text{C}$.

MUC1-Thr4: HGVT*SAPDTRPAPGSTAPPA

MUC1-Thr9: HGVTAPDT*RPAPGSTAPPA

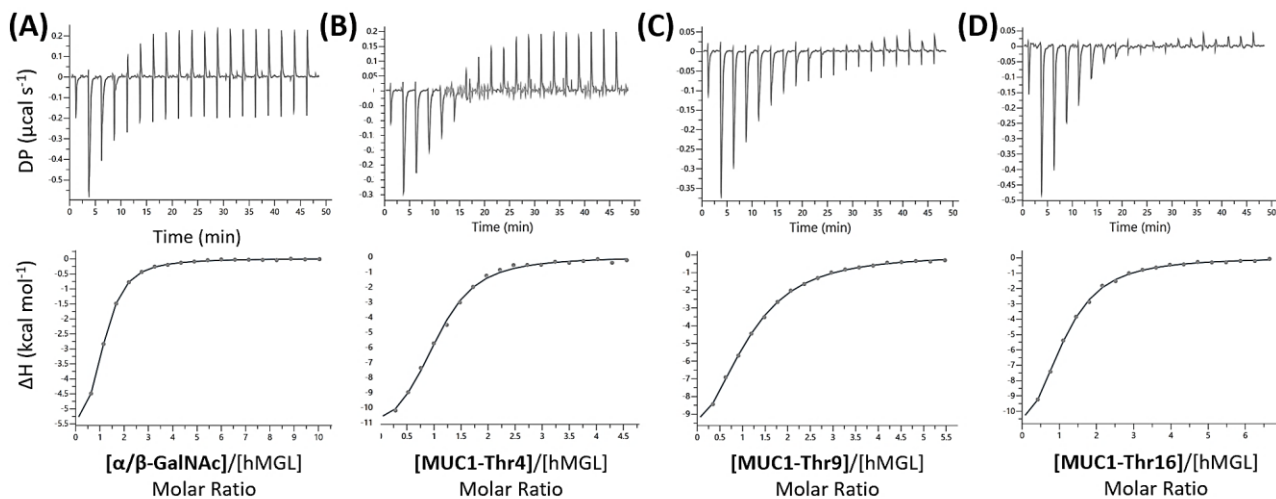
MUC1-Thr16: HGVTAPDTRPAPGST*APPA

MUC1-Thr9,16: HGVTAPDT*RPAPGST*APPA

MUC1-Thr4,16: HGVT*SAPDTRPAPGST*APPA

MUC1-Thr4,9: HGVT*SAPDT*RPAPGSTAPPA

MUC1-Thr4,9,16: HGVT*SAPDT*RPAPGST*APPA

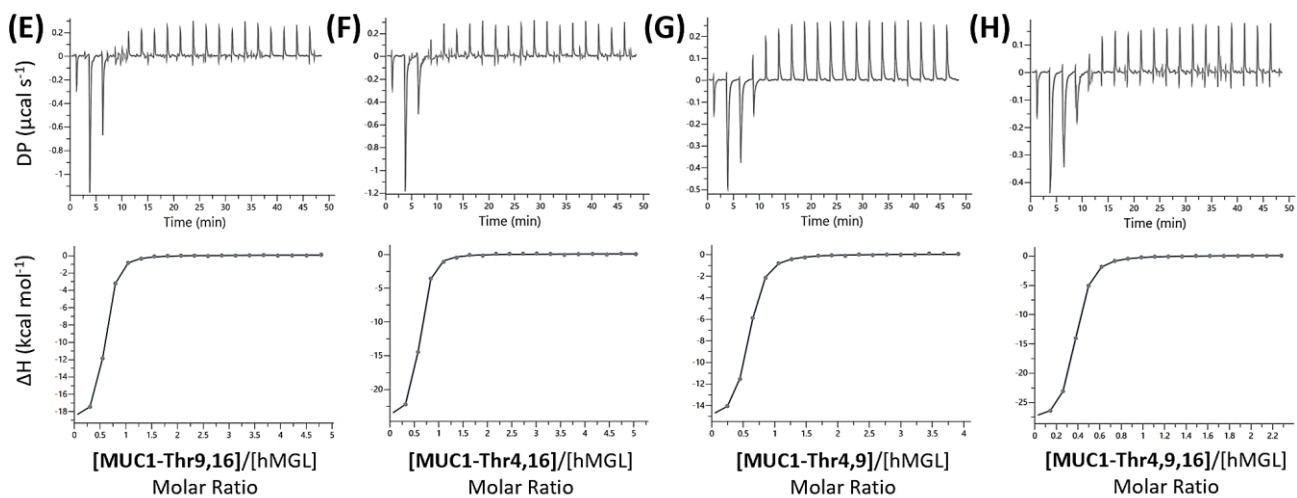


n	0.97
K_s (10^4 M^{-1})	13.79
ΔH (kcal/mol)	-6.81 ± 0.10
$-\Delta S$ (kcal/mol)	-0.20
K_d (μM)	7.25 ± 0.02

n	1.00
K_s (10^4 M^{-1})	26.88
ΔH (kcal/mol)	-12.50 ± 0.50
$-\Delta S$ (kcal/mol)	5.13
K_d (μM)	3.72 ± 0.47

n	1.01
K_s (10^4 M^{-1})	10.84
ΔH (kcal/mol)	-14.10 ± 0.55
$-\Delta S$ (kcal/mol)	7.22
K_d (μM)	9.22 ± 0.61

n	1.01
K_s (10^4 M^{-1})	16.75
ΔH (kcal/mol)	-14.18 ± 0.63
$-\Delta S$ (kcal/mol)	7.63
K_d (μM)	5.97 ± 0.48

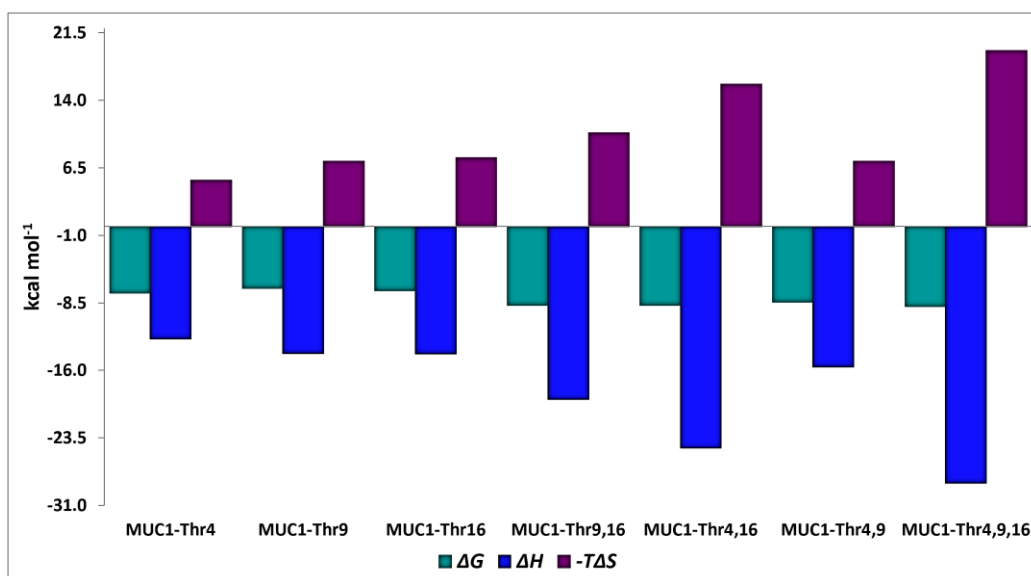


n	0.49
K_a (10^4 M^{-1})	263.15
ΔH (kcal/mol)	-19.20 ± 0.01
$-\Delta S$ (kcal/mol)	10.40
K_d (μM)	0.38 ± 0.01

n	0.50
K_a (10^4 M^{-1})	263.15
ΔH (kcal/mol)	-24.60 ± 0.17
$-\Delta S$ (kcal/mol)	15.80
K_d (μM)	0.38 ± 0.02

n	0.50
K_a (10^4 M^{-1})	144.50
ΔH (kcal/mol)	-15.60 ± 0.01
$-\Delta S$ (kcal/mol)	7.22
K_d (μM)	0.69 ± 0.03

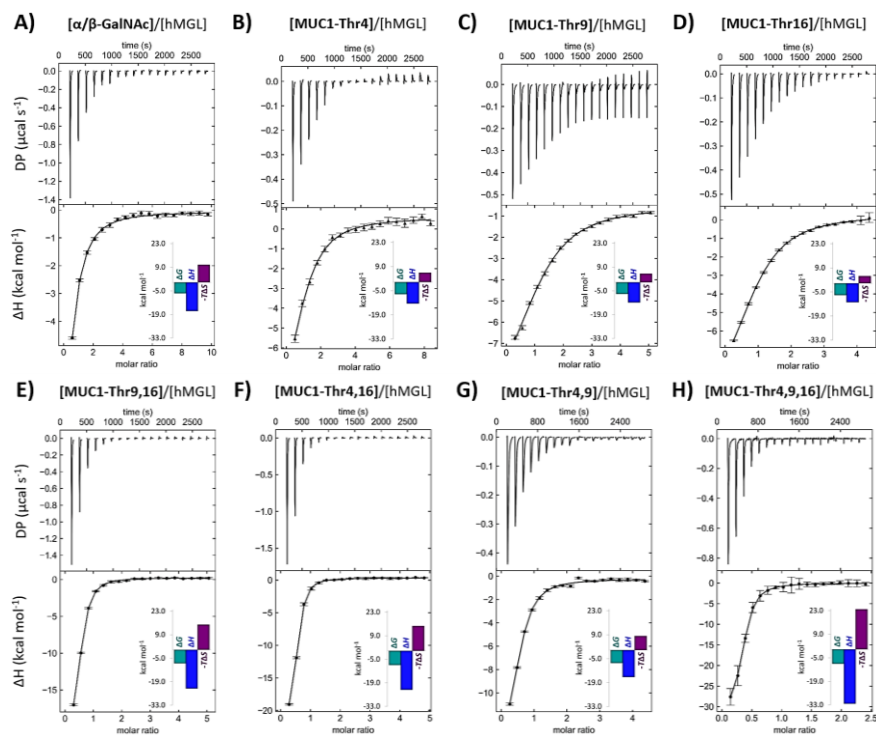
n	0.32
K_a (10^4 M^{-1})	338.98
ΔH (kcal/mol)	-28.50 ± 0.01
$-\Delta S$ (kcal/mol)	19.50
K_d (μM)	0.29 ± 0.01



NITPIC, SEDPHAT, and GUSSI

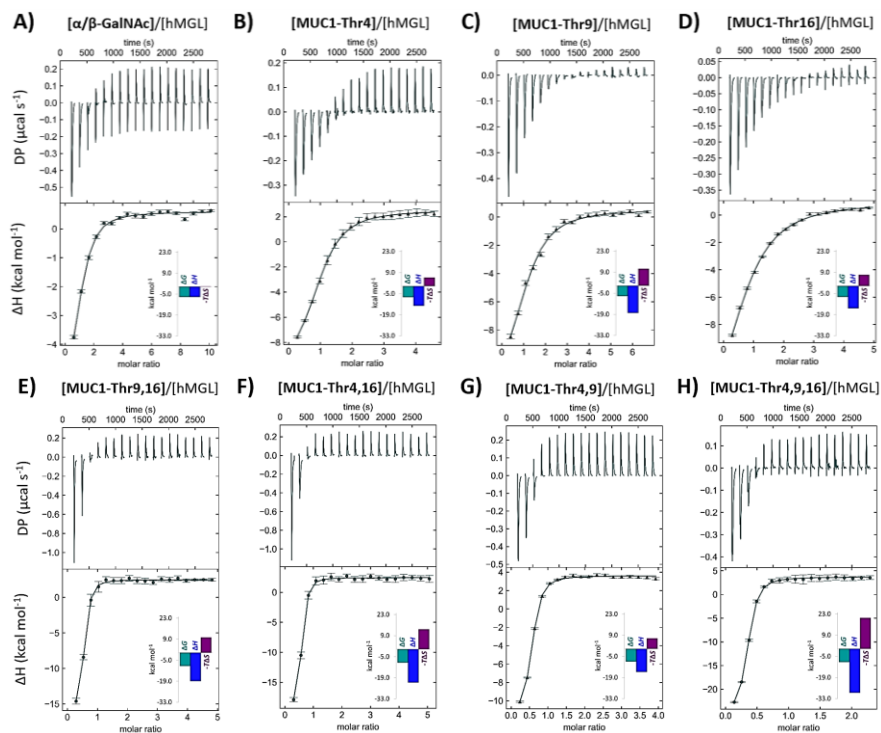
Figure S31. NITPIC/SEDPHAT/GUSSI thermodynamic values in water. Thermodynamics of MUC1 glycopeptide-hMGL interactions. Isotherms corresponding to binding of (A) α/β -GalNAc (1.50 mM) with hMGL (29.6 μ M), (B) MUC1-Thr4 (0.50 mM) with hMGL (11.5 μ M), (C) MUC1-Thr9 (0.44 mM) with hMGL (19.0 μ M), (D) MUC1-Thr16 (0.50 mM) with hMGL (22.0 μ M), (E) MUC1-Thr9,16 (0.50 mM) with hMGL (19.0 μ M), (F) MUC1-Thr4,16 (0.50 mM) with hMGL (20.0 μ M), (G) MUC1-Thr4,9 (0.50 mM) with hMGL (22.0 μ M), and (H) MUC1-Thr4,9,16 (0.25 mM) with hMGL (20.0 μ M). Monte-Carlo error analysis.

Ligand	Entry	K_a $\times 10^4 \text{ M}^{-1}$	ΔG kcal mol^{-1}	ΔH kcal mol^{-1}	$-T\Delta S$ kcal mol^{-1}	n	K_d μM	χ^2
GalNAc		5.23 $\pm 1.08\text{e-}3$	-6.44	-16.88 $\pm 7.49\text{e-}2$	10.44	0.96	19.11	0.416
MUC1-Thr4	7	12.89 $\pm 4.61\text{e-}4$	-6.97	-12.38 $\pm 1.20\text{e-}2$	5.41	0.91	8.90	0.321
MUC1-Thr9	8	10.25 $\pm 7.28\text{e-}4$	-6.83	-11.82 $\pm 4.79\text{e-}3$	4.99	1.17	9.75	0.351
MUC1-Thr16	9	10.27 $\pm 7.27\text{e-}5$	-6.83	-11.01 $\pm 1.00\text{e-}3$	4.17	0.91	11.30	0.129
MUC1-Thr9,16	10	78.18 $\pm 1.78\text{e-}5$	-8.04	-23.06 $\pm 3.19\text{e-}4$	15.03	0.46	2.80	0.444
MUC1-Thr4,16	11	135.20 $\pm 1.26\text{e-}5$	-8.36	-2.11 $\pm 1.13\text{e-}4$	14.72	0.47	1.50	0.212
MUC1-Thr4,9	12	33.97 $\pm 2.88\text{e-}5$	-7.54	-15.77 $\pm 4.56\text{e-}4$	8.22	0.49	2.94	1.24
MUC1-Thr4,9,16	13	163.80 $\pm 6.29\text{e-}5$	-8.47	-32.26 $\pm 1.11\text{e-}3$	23.78	0.33	0.61	0.034



NITPIC/SEDPHAT/GUSSI thermodynamic values in deuterium oxide. Thermodynamics of MUC1 glycopeptide-hMGL interactions. Isotherms corresponding to binding of (A) α/β -GalNAc (1.50 mM) with hMGL (28.6 μ M), (B) MUC1-Thr4 (0.50 mM) with hMGL (21.0 μ M), (C) MUC1-Thr9 (0.44 mM) with hMGL (17.5 μ M), (D) MUC1-Thr16 (0.50 mM) with hMGL (14.4 μ M), (E) MUC1-Thr9,16 (0.50 mM) with hMGL (20.0 μ M), (F) MUC1-Thr4,16 (0.50 mM) with hMGL (19.0 μ M), (G) MUC1-Thr4,9 (0.50 mM) with hMGL (24.5 μ M), and (H) MUC1-Thr4,9,16 (0.25 mM) with hMGL (21.0 μ M). Monte-Carlo error analysis.

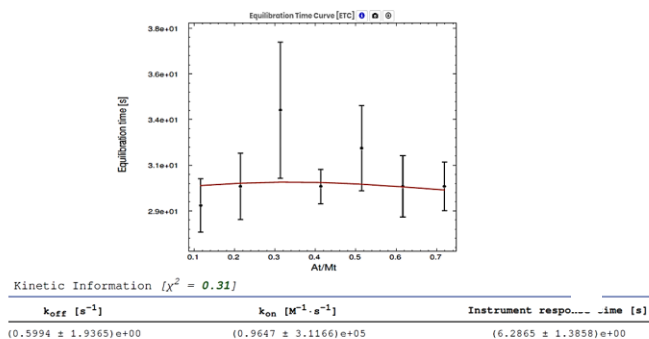
Ligand	Entry	K_a $\times 10^4 \text{ M}^{-1}$	ΔG kcal mol^{-1}	ΔH kcal mol^{-1}	$-T\Delta S$ kcal mol^{-1}	n	K_d μM	χ^2
GalNAc		11.45 $\pm 3.36\text{e-}4$	-6.90	-6.91 $\pm 3.30\text{e-}3$	0.01	0.97	8.60	1.11
MUC1-Thr4	7	23.59 $\pm 1.22\text{e-}4$	-7.33	-13.01 $\pm 1.00\text{e-}3$	5.68	0.96	3.70	0.156
MUC1-Thr9	8	9.89 $\pm 1.76\text{e-}4$	-6.82	-18.02 $\pm 5.79\text{e-}3$	11.21	0.82	12.60	0.942
MUC1-Thr16	9	19.47 $\pm 4.67\text{e-}4$	-7.22	-14.74 $\pm 2.11\text{e-}3$	7.33	1.07	5.50	0.646
MUC1-Thr9,16	10	265.90 $\pm 3.60\text{e-}5$	-8.77	-18.86 $\pm 1.40\text{e-}4$	10.10	0.47	0.38	0.126
MUC1-Thr4,16	11	325.70 $\pm 2.52\text{e-}5$	-8.89	-22.13 $\pm 1.01\text{e-}4$	13.25	0.44	0.62	0.185
MUC1-Thr4,9	12	136.80 $\pm 9.53\text{e-}6$	-8.37	-15.26 $\pm 5.34\text{e-}5$	6.88	0.50	1.40	0.996
MUC1-Thr4,9,16	13	257.00 $\pm 2.33\text{e-}5$	-8.75	-29.11 $\pm 3.50\text{e-}4$	20.37	0.32	1.10	0.159



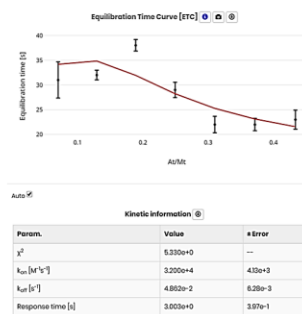
AFFINImeter KinITC

Figure S32. Affinimeter KinITC data in water.

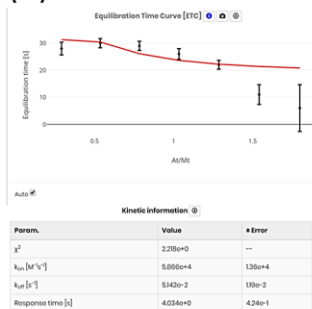
(A) MUC1-Thr16 (9)



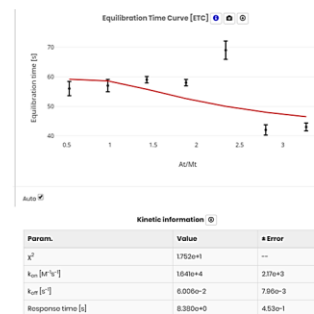
(B) MUC1-Thr9,16 (10)



(C) MUC1-Thr4,16 (11)



(D) MUC1-Thr4,9 (12)



(E) MUC1-Thr4,9,16 (13)

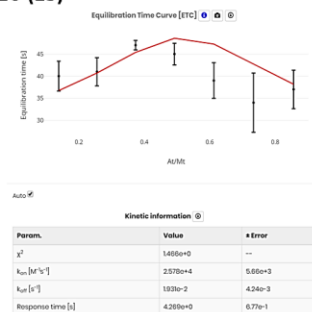
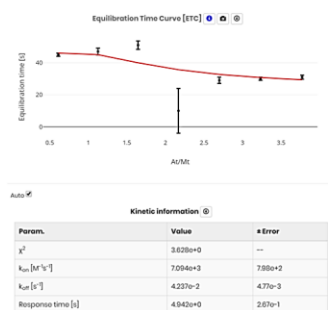


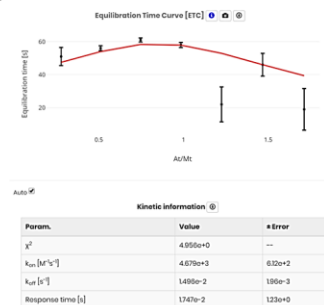
Figure S33. AFFINImeter KinITC data in deuterium.

Ligand	Entry	k_{on} $\times 10^6 M^{-1} s^{-1}$	k_{off} s^{-1}	τ s
D_2O				
GalNAc		0.0070	0.0423	23.60
MUC1-Thr4	7	0.0046	0.0149	66.84
MUC1-Thr9	8	-	-	-
MUC1-Thr16	9	-	-	-
MUC1-Thr9,16	10	-	-	-
MUC1-Thr4,16	11	0.0446	0.0058	172.41
MUC1-Thr4,9	12	0.0257	0.0203	49.06
MUC1-Thr4,9,16	13	0.0351	0.0162	61.72

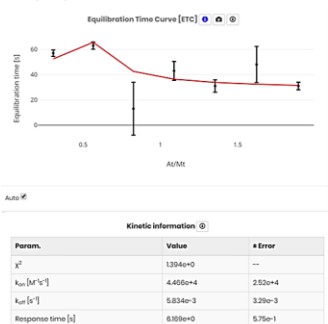
(A) α/β -GalNAc



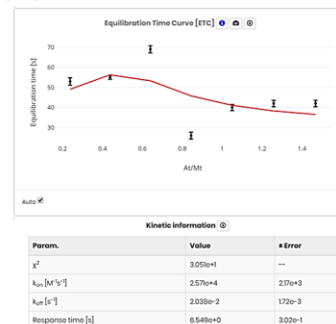
(B) MUC1-Thr4 (7)



(C) MUC1-Thr4,16 (11)



(D) MUC1-Thr4,9 (12)



(E) MUC1-Thr4,9,16 (13)

